arXiv:1406.0089v3 [cs.DC] 20 Aug 2015

RECURSIVE ALGORITHMS FOR DISTRIBUTED FORESTS OF OCTREES

TOBIN ISAAC*, CARSTEN BURSTEDDE†, LUCAS C. WILCOX‡, AND OMAR GHATTAS*§¶

Abstract. The forest-of-octrees approach to parallel adaptive mesh refinement and coarsening (AMR) has recently been demonstrated in the context of a number of large-scale PDE-based applications. Efficient reference software has been made freely available to the public both in the form of the standalone `p4est` library and more indirectly by the general-purpose finite element library `deal.II`, which has been equipped with a `p4est` backend.

Although linear octrees, which store only leaf octants, have an underlying tree structure by definition, it is not fully exploited in previously published mesh-related algorithms. This is because tree branches are not explicitly stored, and because the topological relationships in meshes, such as the adjacency between cells, introduce dependencies that do not respect the octree hierarchy. In this work we combine hierarchical and topological relationships between octants to design efficient recursive algorithms that operate on distributed forests of octrees.

We present three important algorithms with recursive implementations. The first is a parallel search for leaves matching any of a set of multiple search criteria, such as leaves that contain points or intersect polytopes. The second is a ghost layer construction algorithm that handles arbitrarily refined octrees that are not covered by previous algorithms, which require a 2:1 condition between neighboring leaves. The third is a universal mesh topology iterator. This iterator visits every cell in a partition, as well as every interface (face, edge and corner) between these cells. The iterator calculates the local topological information for every interface that it visits, taking into account the nonconforming interfaces that increase the complexity of describing the local topology. To demonstrate the utility of the topology iterator, we use it to compute the numbering and encoding of higher-order C^0 nodal basis functions used for finite elements.

We analyze the complexity of the new recursive algorithms theoretically, and assess their performance, both in terms of single-processor efficiency and in terms of parallel scalability, demonstrating good weak and strong scaling up to 458k cores of the JUQUEEN supercomputer.

Key words. forest of octrees, parallel adaptive mesh refinement, Morton code, recursive algorithms, large-scale scientific computing

AMS subject classifications. 65M50, 68W10, 65Y05, 65D18

1. Introduction.

The development of efficient and scalable parallel algorithms that modify computational meshes is necessary for resolving features in large-scale simulations. These features may vanish and reappear, and/or evolve in shape and location, which stresses the dynamic and in-situ aspects of adaptive mesh refinement and coarsening (AMR). Both stationary and time-dependent simulations benefit from flexible and fast remeshing and repartitioning capabilities, for example when using a-posteriori error estimation, building mesh hierarchies for multilevel solvers for partial differential equations (PDEs), or tracking of non-uniformly distributed particles by using an underlying adaptive mesh.

Three main algorithmic approaches to AMR have emerged over time, which we may call unstructured (U), block-structured (S), and hierarchical or tree-based (T) AMR. Just some examples that integrate parallel processing are (U) [16, 21, 30], (S) [7, 12, 17, 18], and (T) [22, 27, 28]. While these approaches have been developed independently of one another, there has been a definite crossover of key technologies.

*Institute for Computational Engineering and Sciences, The University of Texas at Austin, USA
†Institut für Numerische Simulation, Rheinische Friedrich-Wilhelms-Universität Bonn, Germany
‡Department of Applied Mathematics, Naval Postgraduate School, USA
§Jackson School of Geosciences, The University of Texas at Austin, USA
¶Department of Mechanical Engineering, The University of Texas at Austin, USA

The graph-based partitioning algorithms traditionally used in UAMR have for instance been supplemented by fast algorithms based on coordinate partitioning and space-filling curves (SFCs) [9]. Hierarchical ideas and SFCs have also been applied in SAMR packages to speed up and improve the partitioning [8, 10]. Last but not least, the unstructured meshing paradigm can be employed to create a root mesh of connected trees when a nontrivial geometry needs to be meshed by forest-of-octrees TAMR [3, 6, 26].

The three approaches mentioned above differ in the way that the mesh topology information is passed to applications. With UAMR, the mesh is usually stored in memory as an adjacency graph, and the application traverses the graph to compute residuals, assemble system matrices, etc. This approach has the advantages that local graph traversal operations typically have constant runtime complexity and that the AMR library can remain oblivious of the details of the application, but the disadvantages of less efficient global operations, such as locating the cell containing a point, and of unpredictable memory access. On the other hand, the SAMR approach allows for common operations to be optimized and to use regular memory access patterns, but requires more integration between the AMR package and the application, which may not have access to the topology in a way not anticipated by the AMR package.

Tree-based AMR can be integrated with an application for convenience [24], but can also be kept strictly modular [28]. Most TAMR packages implement logarithmic-complexity algorithms for both global operations, such as point location, and local operations, such as adjacency queries. The paper [6] introduces the `p4est` library, which implements distributed forest-of-octree AMR with an emphasis on geometric and topological flexibility and parallel scalability, and connects with applications through a minimal interface.

The implementation of `p4est` does not explicitly build a tree data structure, so tree-based, recursive algorithms are largely absent from the original presentation in [6]. Many topological operations on octrees and quadtrees, however, are naturally expressed as recursive algorithms, which have simple descriptions and often have good, cache-oblivious memory access patterns. In this paper, we present, analyze, and demonstrate the efficiency of algorithms for important hierarchical and topological operations: searching for leaves matching multiple criteria in parallel, identifying neighboring (ghost) domains from minimal information, and iterating over mesh cells and interfaces. We include an example algorithm that uses this iteration to create a high-order finite element node numbering. Each algorithm has a key recursive component that gives it an advantage over previously developed non-recursive algorithms, such as improved efficiency, coverage of additional use cases, or both. We demonstrate the per-process efficiency of these algorithms, as well as their parallel scalability, on the full size of JUQUEEN [15], a Blue Gene/Q [13] supercomputer.

2. Forest of octree types and operations. Here we present the important concepts on which we build our algorithms. We review the data structures for octants and distributed forests of octrees that were presented in [6]. We also define a data type to handle both octants and octant boundaries that will allow us to describe the topology of forests of octrees.[1] The definitions in this section are summarized in Table 2.1. For the sake of correctness, the definitions in this section are given formally, but the reader may find that the figures are just as helpful in understanding

[1] This data type is a notational convenience for this work, not part of the `p4est` interface.

TABLE 2.1
A summary of Section 2 and the locations of the definitions in the text.

	§ 2.1 Octants and points	
octant $\mathtt{o}$, dom($\mathtt{o}$)	Data type and the cube in $\mathbb{R}^d$ it represents	(2.1)
root(t)	Root of the t-th octree: side length $2^{l_{\max}}$	(2.2)
atom $\mathtt{a}$	level-$l_{\max}$ octant: side length 1	
$\{\mathrm{dom}_b(\mathtt{o})\}_{b\in\mathcal{B}\cup\{v_0\}}$	Octant boundary domains and their indices	Fig. 2.1
point $\mathtt{c} = (\mathtt{o}, b)$	Common data type for octants and interfaces	
dom($\mathtt{c}$)	A point's n-dim. ($n \le d$) hypercube domain	(2.3)
dim($\mathtt{c}$)	Topological dimension of a point	
level($\mathtt{c}$)	Refinement level for points	(2.4)
	§ 2.2 Hierarchical and topological relationships	
desc($\mathtt{c}$)	Descendants of point $\mathtt{c}$	(2.5)
child($\mathtt{c}$)	Children of point $\mathtt{c}$ (Table 2.2, 3rd column)	(2.6)
part($\mathtt{c}$)	Child partition of point $\mathtt{c}$ (", 4th column)	(2.7)
clos($\mathtt{c}$)	Closure set of point $\mathtt{c}$	(2.9)
bound($\mathtt{c}$)	Boundary set of point $\mathtt{c}$ (", 2nd column)	(2.10)
supp($\mathtt{c}$)	Support set of point $\mathtt{c}$ (", 5th column)	(2.11)
atom supp($\mathtt{c}$)	Atomic support set of 0-point $\mathtt{c}$	(2.12)
	§ 2.3 Forests of octrees	
$\mathcal{T} := \{(T^t, \varphi^t)\}_{0\le t<K}$	Conformal macro mesh of Ω	(2.13)
Dom($\mathtt{c}$)	Point domain mapped by φ^t into Ω	(2.14)
$\mathcal{O} := \bigsqcup_{0\le t<K} \mathcal{O}^t$	Non-conformal mesh via octree refinement	(2.15)
	§ 2.4 Distributed forests of octrees	
$\mathtt{o} \le \mathtt{r}$	SFC-based total octant order	Alg. 2.1
$\mathcal{O}_\mathfrak{p} := \bigsqcup_{0\le t<K} \mathbf{O}^t_\mathfrak{p}$	Sorted arrays of leaves owned by $\mathfrak{p}$ for each tree	(2.16)
$\Omega_\mathfrak{p}$, Ω^t, $\Omega^t_\mathfrak{p}$	Subdomains of $\mathcal{O}_\mathfrak{p}$, $\mathcal{O}^t$, $\mathbf{O}^t_\mathfrak{p}$	(2.17)
locate($\mathtt{a}$)	Process $\mathfrak{q}$ such that Dom($\mathtt{a}$) $\subseteq \Omega_\mathfrak{q}$ for atom $\mathtt{a}$	(2.18)
$(\mathtt{f}_\mathfrak{q}, \mathtt{l}_\mathfrak{q}) := \mathrm{range}(\mathfrak{q})$	First and last atoms located in $\Omega_\mathfrak{q}$	(2.19)
$(\mathtt{f}_\mathtt{o}, \mathtt{l}_\mathtt{o}) := \mathrm{range}(\mathtt{o})$	First and last atoms in octant $\mathtt{o}$'s descendants	(2.20)
$\mathbf{f} := \{\mathtt{f}_\mathfrak{q}\}_{0\le\mathfrak{q}<P}$	Sorted array of the first atoms of all processes	(2.21)
$\mathtt{F}_\mathfrak{p} := (\mathcal{T}, \mathcal{O}_\mathfrak{p}, \mathbf{f})$	Distributed forest of octrees	(2.22)

our concepts, as they often correspond to geometrically intuitive ideas.

REMARK 2.1 (Notation). If we have defined an operation op($\cdot$) for every $a \in \mathcal{A}$, then $\mathrm{op}(\mathcal{A}) := \{\mathrm{op}(a) : a \in \mathcal{A}\}$. $|\mathcal{A}|$ is the cardinality of set $\mathcal{A}$. If $\{\mathcal{A}_i\}_{i\in\mathcal{I}}$ are disjoint, their union is written $\bigsqcup_{i\in\mathcal{I}} \mathcal{A}_i$. For a subset A of a manifold, $\overline{A}$, ∂A, and A° are the closure, boundary, and interior of A. We distinguish variable types with fonts:

- standard lower-case for integers and index sets ($a, b, c, \dots$), except for K, N, and P, which are the number of octrees, octants, and processes,
- typewriter for compound data types ($\mathtt{a}, \mathtt{b}, \mathtt{c}, \dots$),
- Fraktur for MPI processes ($\mathfrak{a}, \mathfrak{b}, \mathfrak{c}, \dots$),
- upper-case for subsets of $\mathbb{R}^d$ and manifolds ($A, B, C, \dots$),
- calligraphic for finite sets ($\mathcal{A}, \mathcal{B}, \mathcal{C}, \dots$), and
- bold for finite sets represented as indexable arrays ($\mathbf{A}, \mathbf{B}, \mathbf{C}, \dots$).

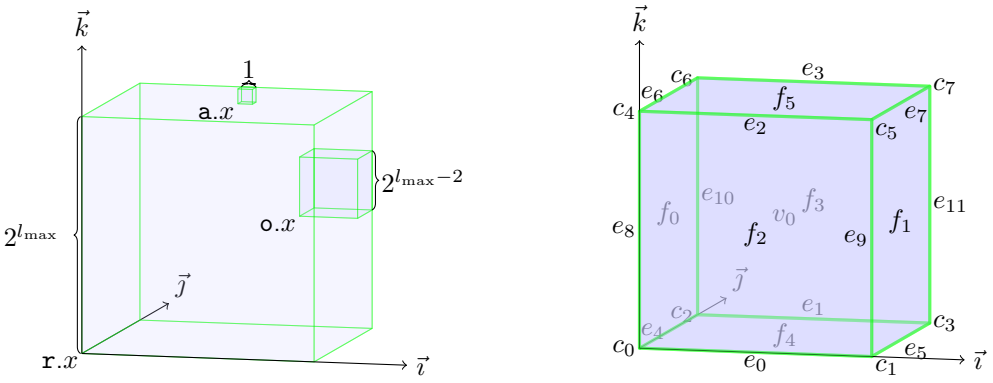

FIG. 2.1. *(left) An illustration of the domains of a root octant* r*, a level-2 octant* o*, and an atom* a*. (right) The correlation between the boundary indices in $\mathcal{B}$ (see the definition at the bottom of this page) and the lower-dimensional hypercubes—squares, line segments, and vertices—in the boundary of an octant, with the central cube labeled with the volume index, v_0 (adapted with permission from [6, Fig. 2]). These indices are used to define points.*

2.1. Octants and points. Here we define the octant data type, which we will use in our algorithms, and some special octants, which are illustrated in Figure 2.1.

An *octant* ($d = 3$) or *quadrant* ($d = 2$) o has the following data fields:

- $\mathtt{o}.t \in \mathbb{N}$—o's *tree index*, relevant to forests of octrees (see Section 2.3);[2]
- $\mathtt{o}.l \in \{0, 1, \ldots, l_{\max}\}$—o's *level of refinement* (or just *level*);
- $\mathtt{o}.x \in \mathbb{Z}^d$—o's *coordinates*, whose components must be multiples of $2^{l_{\max}-\mathtt{o}.l}$.

The fields $\mathtt{o}.l$ and $\mathtt{o}.x$ encode an open cube in $\mathbb{R}^d$—o's *domain*—with sides of length $2^{l_{\max}-\mathtt{o}.l}$,

$$\mathrm{dom}(\mathtt{o}) := \{X \in \mathbb{R}^d : \mathtt{o}.x_i < X_i < \mathtt{o}.x_i + 2^{l_{\max}-\mathtt{o}.l},\ 0 \le i < d\}. \tag{2.1}$$

For every tree index t, the *root* is the level-0 octant whose domain is $(0, 2^{l_{\max}})^d$:

$$\mathrm{root}(t).t := t, \quad \mathrm{root}(t).l := 0, \quad \mathrm{root}(t).x := (0)^d. \tag{2.2}$$

An *atom* a is a smallest-possible octant, which has $\mathtt{a}.l = l_{\max}$ and sides of length 1.

The algorithms we present involve both the hierarchical aspect of octrees and the topological aspect of their domains. Here we define a data type, which we will call a *point*, that encompasses both octants and their interfaces. We will then define topological and hierarchical operations for points in Section 2.2. We present these definitions in the context of a single octree. Minor modifications will be necessary for a forest of octrees, which we will discuss in Section 2.3 (see Remark 2.9).

The boundary of a cube in $\mathbb{R}^d$ has a standard partition into lower-dimensional hypercubes, which contains $2^{d-n}\binom{d}{n}$ n-dimensional hypercubes for $0 \le n < d$: since $(2+1)^d = \sum_{n=0}^{d}\binom{d}{n}2^{d-n}1^n$, there are $3^d - 1$ in all. We index these hypercubes with a set of *boundary indices* $\mathcal{B}$. The *boundary domain* $\mathrm{dom}_b(\mathtt{o})$, $b \in \mathcal{B}$, is the corresponding hypercube in the boundary of $\mathrm{dom}(\mathtt{o})$. For $d = 3$, $\mathcal{B}$ is made of eight corner indices $\{c_i\}_{0\le i<8}$, twelve edge indices $\{e_i\}_{0\le i<12}$, and six face indices $\{f_i\}_{0\le i<6}$, which are all illustrated in Figure 2.1. For convenience, we define one additional index, the *volume index* v_0 corresponding to the volume of an octant, which defines an alias of an octant's domain, $\mathrm{dom}_{v_0}(\mathtt{o}) := \mathrm{dom}(\mathtt{o})$.

[2] In p4est, the tree index is always available from context, not stored with the octant.

A *point* is a tuple $(\mathtt{o}, b)$, where $\mathtt{o}$ is an octant and $b \in \mathcal{B} \cup \{v_0\}$. The *domain of a point* $\mathtt{c} = (\mathtt{o}, b)$ is

$$\mathrm{dom}(\mathtt{c}) := \mathrm{dom}_b(\mathtt{o}). \tag{2.3}$$

Two points are equal if and only if their domains are equal. The *dimension* $\dim(\mathtt{c})$ of a point $\mathtt{c}$ is the topological dimension of its domain. If $\dim(\mathtt{c}) = n$, $\mathtt{c}$ is an *n-point*. The *level* of a point $\mathtt{c}$ is the minimum refinement level of all octants in the vicinity of $\mathtt{c}$ that appear in a point tuple equal to $\mathtt{c}$,

$$\mathrm{level}(\mathtt{c}) := \min\{\mathtt{o}.l : \exists b \in \mathcal{B} \cup \{v_0\},\ (\mathtt{o}, b) = \mathtt{c}\}. \tag{2.4}$$

If $\dim(\mathtt{c}) > 0$, there is no need to use the minimum refinement level in the definition of $\mathrm{level}(\mathtt{c})$, because all octants that have $\mathtt{c}$ as a boundary point have the same refinement level: $(\mathtt{c} = (\mathtt{o}, b)) \Leftrightarrow (\mathrm{level}(\mathtt{c}) = \mathtt{o}.l)$. A 0-point, however, may be a corner point for octants with different refinement levels: by choosing the minimum we make a 0-point's level match that of the biggest neighboring octant.

Remark 2.2. We consider octants to be points: when an operation on a point is applied to an octant $\mathtt{o}$, one should understand $(\mathtt{o}, v_0)$.

2.2. Hierarchical and topological relationships. Here we define the hierarchical and topological relationships used in our algorithms and proofs below. We show what these relationships look like in Table 2.2.

The hierarchical relationships between points are determined by set inclusion of their domains. The *descendants* of a point $\mathtt{c}$ are all of the points with the same dimension whose domains are contained in the domain of $\mathtt{c}$,

$$\mathrm{desc}(\mathtt{c}) := \{\mathtt{e} : \dim(\mathtt{e}) = \dim(\mathtt{c}),\ \mathrm{dom}(\mathtt{e}) \subseteq \mathrm{dom}(\mathtt{c})\}. \tag{2.5}$$

The *children* of a point $\mathtt{c}$ are descendants that are more refined than $\mathtt{c}$ by one level,

$$\mathrm{child}(\mathtt{c}) := \{\mathtt{h} : \mathtt{h} \in \mathrm{desc}(\mathtt{c}),\ \mathrm{level}(\mathtt{h}) = \mathrm{level}(\mathtt{c}) + 1\}. \tag{2.6}$$

The requirement that an octant $\mathtt{o}$'s coordinates must be multiples of $2^{l_{\max} - \mathtt{o}.l}$ has the consequence that the domains of two distinct points with the same level do not overlap, and that every point's domain is tiled by the domains of its children (a collection $\mathcal{U}$ of subsets of a set S in a topological space tiles S if $S \subseteq \bigcup_{U \in \mathcal{U}} \overline{U}$ and $(U, V \in \mathcal{U}, U \neq V) \Rightarrow (U \cap V = \emptyset)$).

Proposition 2.3. *If* $\dim(\mathtt{c}) > 0$*, then* $|\mathrm{child}(\mathtt{c})| = 2^{\dim(\mathtt{c})}$ *and* $\mathrm{dom}(\mathrm{child}(\mathtt{c}))$ *tiles* $\mathrm{dom}(\mathtt{c})$.

A point's domain is tiled by its children's domains, but it is not partitioned by them, as they are open sets. To define a partition, we must add lower-dimensional points between them. The *child partition* is the set of all points whose domains are contained in $\mathrm{dom}(\mathtt{c})$ and whose levels are greater by one,

$$\mathrm{part}(\mathtt{c}) := \{\mathtt{h} : \mathrm{level}(\mathtt{h}) = \mathrm{level}(\mathtt{c}) + 1,\ \mathrm{dom}(\mathtt{h}) \subset \mathrm{dom}(\mathtt{c})\}. \tag{2.7}$$

Proposition 2.4. *If* $\dim(\mathtt{c}) > 0$*, then* $|\mathrm{part}(\mathtt{c})| = 3^{\dim(\mathtt{c})}$ *and* $\mathrm{part}(\mathtt{c})$ *defines a partition,* $\mathrm{dom}(\mathtt{c}) = \bigsqcup \mathrm{dom}(\mathrm{part}(\mathtt{c}))$.

The two basic topological sets we need for a point $\mathtt{c}$ are the lower-dimensional points that surround $\mathtt{c}$—its boundary points—and the octants that surround $\mathtt{c}$—its

TABLE 2.2

For $d = 3$, illustrations of the boundary sets (bound(c))*, children* (child(c))*, child partition sets* (part(c))*, and support sets* (supp(c)) *of octants and lower-dimensional n-points. The closure set, not illustrated, is the union of the point with its boundary set. For a 0-point, the atomic support set* atom supp(c) *looks like the support set, only scaled down.*

n	c	bound(c)	child(c)	part(c)	supp(c)
0	(corner)	$\emptyset$	$\emptyset$	$\emptyset$	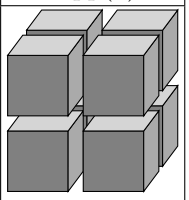
1	(edge)				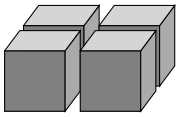
2	(face)				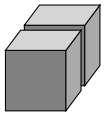
3	(octant)	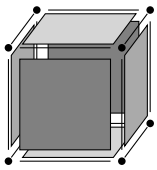	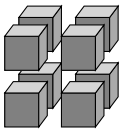	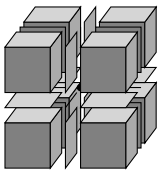	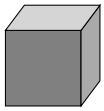

support octants. To define boundary points, we first define closure points. The *closure set of an octant* o is the set of all points in which o may appear in a point tuple,

$$\text{clos}(\mathsf{o}) := \{(\mathsf{o}, b) : b \in \mathcal{B} \cup \{v_0\}\}. \tag{2.8}$$

The *closure set of a point* c is the intersection of all octant closure sets containing c,

$$\text{clos}(\mathsf{c}) := \bigcap \{\text{clos}(\mathsf{o}) : \mathsf{c} \in \text{clos}(\mathsf{o})\}. \tag{2.9}$$

The *boundary set* of a point c is its closure less itself,

$$\text{bound}(\mathsf{c}) := \text{clos}(\mathsf{c}) \backslash \{\mathsf{c}\}. \tag{2.10}$$

PROPOSITION 2.5 (Point closure matches $\mathbb{R}^d$ closure). *The domains of points in* c*'s closure set* clos(c) *partition the closure of its domain,* $\overline{\text{dom}(\mathsf{c})} = \bigsqcup \text{dom}(\text{clos}(\mathsf{c}))$.

The *support set* of a point c is the set of octants with the same refinement level as c whose closures include c,

$$\text{supp}(\mathsf{c}) := \{\mathsf{o} : \mathsf{c} \in \text{clos}(\mathsf{o}), \mathsf{o}.l = \text{level}(\mathsf{c})\}. \tag{2.11}$$

PROPOSITION 2.6 ($\mathbb{R}^d$ intersection implies support intersection). *If* $\mathtt{o}$ *is an octant,* $\mathtt{c}$ *is a point, and* $\overline{\mathrm{dom}(\mathtt{o})} \cap \mathrm{dom}(\mathtt{c}) \neq \emptyset$*, then there exists* $\mathtt{s} \in \mathrm{supp}(\mathtt{c})$ *such that* $\mathtt{s} \in \mathrm{desc}(\mathtt{o})$ *or* $\mathtt{o} \in \mathrm{desc}(\mathtt{s})$.

The following proposition shows the duality between $\mathrm{clos}(\cdot)$ and $\mathrm{supp}(\cdot)$.

PROPOSITION 2.7. *If* $\dim(\mathtt{c}) > 0$*, then* $(\mathtt{o} \in \mathrm{supp}(\mathtt{c})) \Leftrightarrow (\mathtt{c} \in \mathrm{clos}(\mathtt{o}))$.

For 0-points, this duality does not hold because a 0-point can be in the closure set of an octant with a more refined level. In fact, every 0-point is in the closure of an atom. The *atomic support set* of a 0-point $\mathtt{c}$ is the set of atoms whose closures include $\mathtt{c}$,

$$\mathrm{atom\,supp}(\mathtt{c}) := \{\mathtt{a} : \mathtt{c} \in \mathrm{clos}(\mathtt{a}), \mathtt{a}.l = l_{\max}\}. \tag{2.12}$$

The support and atomic support sets of a 0-point contain and are contained in all neighboring octants, respectively.

PROPOSITION 2.8. *If* $\dim(\mathtt{c}) = 0$*,* $\mathtt{o}$ *is a octant, and* $\mathtt{c} \in \mathrm{clos}(\mathtt{o})$*, then there are* $\mathtt{a} \in \mathrm{atom\,supp}(\mathtt{c})$ *and* $\mathtt{s} \in \mathrm{supp}(\mathtt{c})$ *such that* $\mathtt{a} \in \mathrm{desc}(\mathtt{o})$ *and* $\mathtt{o} \in \mathrm{desc}(\mathtt{s})$.

2.3. Forests of octrees. A forest of quadtrees ($d = 2$) or octrees ($d = 3$) is a mesh of a d-dimensional domain Ω with two layers, a macro layer and a micro layer. The *macro layer* is a geometrically conformal mesh[3] of K mapped cells (quadrilaterals ($d = 2$) or hexahedra ($d = 3$)),

$$\mathcal{T} := \{(T^t, \varphi^t)\}_{0 \le t < K}, \tag{2.13}$$

where each T^t has an associated map $\varphi^t : \overline{\mathrm{dom}(\mathrm{root}(t))} \to \overline{T^t}$, which is a continuous bijection between the domain of the root octant and T^t. We define the *mapped domain of a point* $\mathtt{c} = (\mathtt{o}, b)$ by its image under the map for $\mathtt{o}$'s tree index,

$$\mathrm{Dom}(\mathtt{c}) := \varphi^{o.t}(\mathrm{dom}_b(\mathtt{o})). \tag{2.14}$$

REMARK 2.9 (Modifications to definitions for forests). In Section 2.1 we defined points in the context of a single octree. In the forest-of-octrees context, we consider two points equal if their mapped domains are equal. If one substitutes mapped domains for unmapped domains in the definitions and propositions in Section 2.2, they hold in the forest-of-octrees context. If a point $\mathtt{c}$'s mapped domain is on the boundary between macro-layer cells, then $\mathtt{c}$'s support set $\mathrm{supp}(\mathtt{c})$ no longer has the regular shape shown in Table 2.2, but depends on the macro layer topology. A face on the boundary of Ω, for example, has only one support octant. We emphasize that the sets defined in Section 2.2 do not depend on the exact nature of the maps $\{\varphi^t\}_{0 \le t < K}$, but can be constructed, in time proportional to their sizes, from the point data of their arguments and the mesh topology of $\mathcal{T}$, i.e., which cells are neighbors, which of their faces correspond, and how those faces are oriented relative to each other. These issues are covered in [6, Section 2.2].

For each $0 \le t < K$, the *tree-t leaves* $\mathcal{O}^t \subset \mathrm{desc}(\mathrm{root}(t))$ are a set of $N^{(t)}$ octants whose domains tile $\mathrm{dom}(\mathrm{root}(t))$. The *micro layer* $\mathcal{O}$ is the union of these sets, and its size is N,

$$\mathcal{O} := \bigsqcup_{0 \le t < K} \mathcal{O}^t, \; N := |\mathcal{O}| = \sum_{0 \le t < K} N^{(t)}. \tag{2.15}$$

[3]By "geometrically conformal mesh" we mean that $\{T^t\}_{0 \le t < K}$ are the cells of a CW complex (a generalization of simplicial complex to other polytopes, where C stands for closure-finite and W for weak topology; see e.g. [19, Chapter 10]): informally, each T^t is open, $\{T^t\}_{0 \le t < K}$ tiles Ω, and if the intersection $\overline{T^s} \cap \overline{T^t}$ has dimension $(d-1)$, then it is equal to a whole face of T^s and a whole face of T^t.

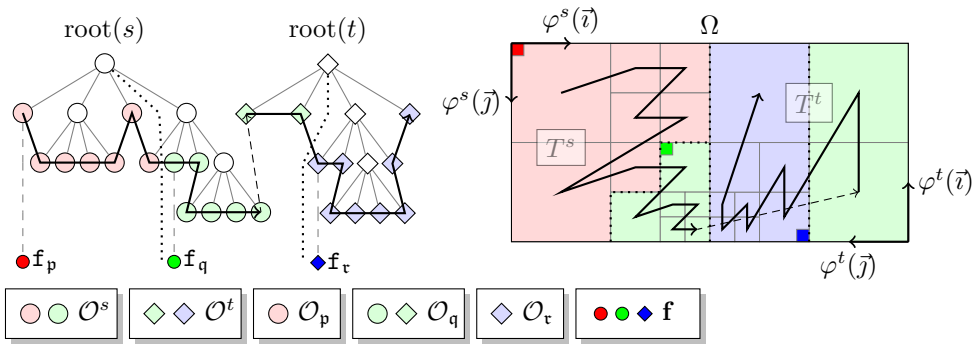

FIG. 2.2. *(Adapted with permission from [6, Fig. 2.1].) A $d = 2$ example of the relationship between the implicit tree structure (left) and the domain tiling (right) of a forest of octrees with two trees s and t. The bijections φ^s and φ^t map the implicit coordinate systems of the unmapped octant domains onto the cells T^s and T^t. The left-to-right traversal of the leaves (black "zig-zag" line) demonstrates the total order (Algorithm 2.1). In this example the forest is partitioned among three processes $\mathtt{p}$, $\mathtt{q}$ and $\mathtt{r}$ by sectioning the leaves into $\mathcal{O}_\mathtt{p}$, $\mathcal{O}_\mathtt{q}$, and $\mathcal{O}_\mathtt{r}$. Color conveys this partition, while the node shapes convey the division of the leaves into the trees $\mathcal{O}^\mathtt{s}$ and $\mathcal{O}^t$. The small, brightly colored nodes represent the first atoms located in each process's subdomains* (2.21).

The mapped domains of the micro layer octants tile Ω, but this tiling is not a geometrically conforming mesh: when neighboring octants have different levels, their faces (and edges if $d = 3$) do not conform to each other. If neighboring octants differ by at most one level, the forest is said to satisfy a 2:1 balance condition [14, 24].

We call $\mathcal{O}^t$ the leaves of octree t because one could build a tree structure, starting with root(t) and using the child($\cdot$) operation, whose leaves would be $\mathcal{O}^t$. The `p4est` library does not store this tree structure in memory. Storing just $\mathcal{O}^t$ is an approach known as a linear octree representation [27].

2.4. Distributed forests of octrees. In `p4est`, the macro layer $\mathcal{T}$ is static and replicated on each process, while the micro layer $\mathcal{O}$ is dynamic—it may be adaptively refined, coarsened, and repartitioned frequently over the life of a forest—and distributed, with each process owning a distinct subset of leaves. We describe the distribution method here, and illustrate it in Figure 2.2.

The partitioning of leaves between processes and the layout of leaves in memory is determined by the total order induced by the comparison operation in Algorithm 2.1. The comparison of coordinates in line 2 is defined by a space-filling curve; the `p4est` library uses the so-called z-ordering which corresponds to the Morton curve [20].

Algorithm 2.1: $\mathtt{o} \leq \mathtt{r}$ (octant $\mathtt{o}$, octant $\mathtt{r}$)

1: **if** $\mathtt{o}.t \neq \mathtt{r}.t$ **then return** $(\mathtt{o}.t \leq \mathtt{r}.t)$ *[If $s < t$, all of octree s's leaves come before t's.]*
2: **if** $\mathtt{o}.x \neq \mathtt{r}.x$ **then return** $(\mathtt{o}.x \leq \mathtt{r}.x)$ *[Coordinates are ordered by SFC index.]*
3: **return** $(\mathtt{o}.l \leq \mathtt{r}.l)$ *[Ancestors precede descendants (preordering).]*

REMARK 2.10. When we index a sorted array of octants ($\mathbf{A}[i]$), children (child($\mathtt{o}$)[i]), or a support set (supp($\mathtt{c}$)[i]), we mean the ith octant with respect to the total order.

Using this total order, each process is assigned a contiguous (with respect to the total order) section of leaves in MPI-rank order. For each $0 \leq t < K$ and $0 \leq \mathtt{p} < P$, the subset of $\mathcal{O}^t$ assigned to process $\mathtt{p}$ is in an array $\mathbf{O}^t_\mathtt{p}$, which has size $N^{(t)}_\mathtt{p}$; these

arrays form a partition, $\mathcal{O}^t = \bigsqcup_{0\le \mathtt{p}<P} \mathbf{O}^t_{\mathtt{p}}$. The set of all leaves assigned to $\mathtt{p}$ is

$$\mathcal{O}_{\mathtt{p}} := \bigsqcup_{0\le t<K} \mathbf{O}^t_{\mathtt{p}}; \tag{2.16}$$

its size is $N_{\mathtt{p}} := |\mathcal{O}_{\mathtt{p}}| = \sum_{0\le t<K} N^{(t)}_{\mathtt{p}} > 0$.[4] The *subdomain* of Ω tiled by $\mathrm{Dom}(\mathbf{O}^t_{\mathtt{p}})$ is the interior of its closure,

$$\Omega^t_{\mathtt{p}} := \left(\overline{\bigcup \mathrm{Dom}(\mathbf{O}^t_{\mathtt{p}})}\right)^{\circ}; \tag{2.17}$$

the subdomains Ω^t and $\Omega_{\mathtt{p}}$ are analogously defined.

Because the leaves are partitioned, process $\mathtt{p}$ cannot determine (without communication) if an octant $\mathtt{o}$, whose mapped domain $\mathrm{Dom}(\mathtt{o})$ is outside $\Omega_{\mathtt{p}}$, is a leaf. We do, however, want $\mathtt{p}$ to be able to locate the subdomains that overlap $\mathrm{Dom}(\mathtt{o})$. To allow this, each process in `p4est` has some information about other processes' subdomains, which we describe here. We start from the fact that an atom's mapped domain is *located* in the subdomain of only one process's subdomain,

$$(\mathrm{locate}(\mathtt{a}) := \mathtt{q}) \Leftrightarrow (\mathrm{Dom}(\mathtt{a}) \subseteq \Omega_{\mathtt{q}}). \tag{2.18}$$

Note that $\mathtt{q} = \mathrm{locate}(\mathtt{a})$ does not imply $\mathtt{a} \in \mathcal{O}_{\mathtt{q}}$: $\mathtt{a}$ could be a descendant of a leaf in $\mathcal{O}_{\mathtt{q}}$. To test whether $\mathtt{q} = \mathrm{locate}(\mathtt{a})$ for an arbitrary atom $\mathtt{a}$, it is only necessary to precompute a process's *range*: a tuple of its *first atom* $\mathtt{f}_{\mathtt{q}}$ and its *last atom* $\mathtt{l}_{\mathtt{q}}$ with respect to the total order of octants,

$$\begin{aligned} \mathtt{f}_{\mathtt{q}} &:= \min\{\mathtt{a} : \mathtt{a}.l = l_{\max},\ \mathrm{Dom}(\mathtt{a}) \subseteq \Omega_{\mathtt{q}}\}, \\ \mathtt{l}_{\mathtt{q}} &:= \max\{\mathtt{a} : \mathtt{a}.l = l_{\max},\ \mathrm{Dom}(\mathtt{a}) \subseteq \Omega_{\mathtt{q}}\}, \\ \mathrm{range}(\mathtt{q}) &:= (\mathtt{f}_{\mathtt{q}},\ \mathtt{l}_{\mathtt{q}}). \end{aligned} \tag{2.19}$$

Proposition 2.11. $(\mathtt{q} = \mathrm{locate}(\mathtt{a})) \Leftrightarrow (\mathtt{f}_{\mathtt{q}} \le \mathtt{a} \le \mathtt{l}_{\mathtt{q}})$.

Proposition 2.12 (A range describes a subdomain). $\overline{\Omega_{\mathtt{q}}} = \overline{\bigcup \mathrm{Dom}([\mathtt{f}_{\mathtt{q}}, \mathtt{l}_{\mathtt{q}}])}$, *where* $[\mathtt{f}_{\mathtt{q}}, \mathtt{l}_{\mathtt{q}}]$ *is the set of all atoms* $\mathtt{a}$ *such that* $\mathtt{f}_{\mathtt{q}} \le \mathtt{a} \le \mathtt{l}_{\mathtt{q}}$.

We also apply the range operator to individual octants: the *range of an octant* $\mathtt{o}$ is a tuple of the first and last atoms, $\mathtt{f}_{\mathtt{o}}$ and $\mathtt{l}_{\mathtt{o}}$, in its descendants,

$$\begin{aligned} \mathtt{f}_{\mathtt{o}} &:= \min\{\mathtt{a} :\ \mathtt{a}.l = l_{\max},\ \mathtt{a} \in \mathrm{desc}(\mathtt{o})\}, \\ \mathtt{l}_{\mathtt{o}} &:= \max\{\mathtt{a} :\ \mathtt{a}.l = l_{\max},\ \mathtt{a} \in \mathrm{desc}(\mathtt{o})\}, \\ \mathrm{range}(\mathtt{o}) &:= (\mathtt{f}_{\mathtt{o}},\ \mathtt{l}_{\mathtt{o}}). \end{aligned} \tag{2.20}$$

Proposition 2.13. $(\mathrm{Dom}(\mathtt{o}) \subseteq \Omega_{\mathtt{q}}) \Leftrightarrow (\mathtt{q} = \mathrm{locate}(\mathtt{f}_{\mathtt{o}}) = \mathrm{locate}(\mathtt{l}_{\mathtt{o}}))$.

To locate atoms, it is not necessary to store both $\mathtt{f}_{\mathtt{q}}$ and $\mathtt{l}_{\mathtt{q}}$: $\mathtt{l}_{\mathtt{q}}$ can be computed from $\mathtt{f}_{\mathtt{q}+1}$. In `p4est`, we store a sorted array called the *first-atoms array* $\mathbf{f}$, where

$$\mathbf{f}[\mathtt{p}] := \mathtt{f}_{\mathtt{p}},\ 0 \le \mathtt{p} < P, \tag{2.21}$$

and $\mathbf{f}[P]$ is a phony "terminal" octant whose tree index is K. This array is shown in Figure 2.2. The first atom $\mathtt{f}_{\mathtt{q}}$ is independent of the leaves in $\mathcal{O}_{\mathtt{q}}$, so $\mathbf{f}$ is up-to-date

[4] In `p4est` partitions may be empty, but for simplicity we assume here that they are all non-empty.

even if other processes have refined or coarsened their leaves. Using $\mathbf{f}$, a process can compute locate($\mathtt{a}$) in $O(\log P)$ time and test ($\mathtt{q} = $ locate($\mathtt{a}$)?) in $O(1)$ time.

For the purposes of this paper, we have described all components of a *distributed forest of octrees*, which is, for process $\mathtt{p}$, the combination of macro layer (2.13), local leaves (2.16), and the first-atoms array (2.21),

$$\mathtt{F_p} := (\mathcal{T}, \mathcal{O}_\mathtt{p}, \mathbf{f}). \tag{2.22}$$

REMARK 2.14. $\mathtt{F_p}$ is an assumed argument of the algorithms we present.

3. Parallel multiple-item search via array splitting. We can optimize the search for a leaf that matches a given condition if we begin at the root of an octree and recursively descend to all children that could possibly be a match. This is a lazy exclusion principle which is motivated by a practical consideration: Often an over-optimistic approximate check can be significantly faster than an exact check, which applies to bounding-box checks in computational geometry or to checking the surrounding sphere of a nonlinearly warped octant volume in space.

3.1. Searching in a single octree and in a forest. We assume that the user has a set of arbitrary matching queries indexed by $\mathcal{Q}$: For each $q \in \mathcal{Q}$, match$_q()$ returns true or false for any given octant $\mathtt{o} \in \mathcal{O}$. We also pass a boolean parameter to match$_q()$ that specifies whether $\mathtt{o}$ is a leaf or not. This may be used to execute over-optimistic, cheap matches for non-leaves and strict matches for leaves. This approach is more general than searching for a single leaf that matches each query: Our framework encompasses, for example, the search for all the leaves that intersect a set of polytopes (indexed by $\mathcal{Q}$) embedded in Ω. More generally, it is entirely legal that one leaf matches multiple queries, or one query matches multiple leaves.

In `Search` (Algorithm 3.1), we use recursion and lazy exclusion to track multiple simultaneous queries during one traversal. At each recursion into children we only retain the queries that have returned a possible match on the previous level. We implement this by passing as a callback a user-defined *lazy matching function* `Match`, which is a boolean operator that takes as arguments an octant $\mathtt{o}$, a boolean isLeaf that indicates if $\mathtt{o} \in \mathcal{O}$, and a query index $q \in \mathcal{Q}$ and satisfies the following properties:

- `Match`($\mathtt{o}$, isLeaf, q) returns true if there is a leaf $\mathtt{r} \in \mathcal{O}$ that is a descendant of $\mathtt{o}$ such that match$_q(\mathtt{r})$ = true, and is allowed to return a false positive (i.e., true even if match$_q(\mathtt{r})$ is false for all descendant leaves of $\mathtt{o}$);
- if isLeaf = true, then the return value of `Match` is irrelevant. The functionality of the algorithm resides in the action of the user-defined callback, which is expected to execute appropriate code for strictly matched leaves.

To extend the action of `Search` to the whole forest, it can be called once for each tree index $0 \le t \le K$ with $\mathbf{O}^t_\mathtt{p}$ and root(t) as arguments. The resulting algorithm is communication-free and every leaf is queried on only one process, although the ancestors of leaves may appear as arguments to `Match` for multiple processes.

3.2. Array splitting. `Search` requires an algorithm `Split_array` that we have not yet specified. `Split_array` takes a sorted array of leaves $\mathbf{A}$ and an octant $\mathtt{a}$ such that each leaf $\mathbf{A}[j]$ is a descendant of $\mathtt{a}$ and partitions $\mathbf{A}$ into sorted arrays $\mathbf{H}[0]$, $\mathbf{H}[1]$, $\ldots$, $\mathbf{H}[2^d - 1]$ such that $\mathbf{H}[i]$ contains the descendants of child($\mathtt{a}$)[i].

Because $\mathbf{A}$ is sorted, the subarrays can be indicated by a non-decreasing sequence of indices $0 = \mathbf{k}[0] \le \mathbf{k}[1] \le ... \le \mathbf{k}[2^d] = |\mathbf{A}|$, such that $\mathbf{H}[i] = \mathbf{A}[\mathbf{k}[i], \ldots, \mathbf{k}[i+1] - 1]$. If child($\mathtt{a}$)[$i$] has no descendants in $\mathbf{A}$, this is indicated by $\mathbf{k}[i] = \mathbf{k}[i+1]$.

Algorithm 3.1:
`Search` (octant array $\mathbf{A}$, octant `a`, index set $\mathcal{Q}$, callback `Match`)

Input : $\mathbf{A}$ is a sorted subset of leaves, $\mathbf{A} \subseteq \mathcal{O}$;
`a` is an ancestor of $\mathbf{A}[j]$ for each j, $\mathbf{A} \subseteq \text{desc}(\texttt{a})$.
Result : $\forall q \in \mathcal{Q}$, $\text{match}_q(\texttt{o})$ is called for all leaves o
whose ancestors `a` have also returned true from $\text{match}_q(\texttt{a})$.

1: **if** $\mathbf{A} = \emptyset$ **then return**
2: boolean isLeaf $\leftarrow (\mathbf{A} = \{\texttt{a}\})$
3: index set $\mathcal{Q}_{\text{match}} \leftarrow \emptyset$ *[queries that pass the lazy criteria at* `a`*]*
4: **for all** $q \in \mathcal{Q}$ **do**
5: **if** `Match` (`a`, isLeaf, q) **then** $\mathcal{Q}_{\text{match}} \leftarrow \mathcal{Q}_{\text{match}} \cup \{q\}$ *[*`Match` *runs user action for leaves]*
6: **if** $\mathcal{Q}_{\text{match}} \neq \emptyset$ **and not** isLeaf **then**
7: $\mathbf{H} \leftarrow$ `Split_array` ($\mathbf{A}$, `a`) *[divide* $\mathbf{A}$ *between the children of* `a`*: see Section 3.2]*
8: **for all** $0 \leq i < 2^d$ **do** `Search` ($\mathbf{H}[i]$, child(`a`)$[i]$, $\mathcal{Q}_{\text{match}}$, `Match`)

Let us assume that the children of `a` have level l. If we know that an octant `o` is a descendant of child(`a`)$[i]$ for some i, then we can compute i from `o`.x using Algorithm 3.2, which works because we use the Morton order as our space-filling curve. We call this algorithm `Ancestor_id`, because it is a simple generalization of the algorithm `Child_id` [6, Algorithm 1].

Algorithm 3.2: `Ancestor_id` (octant `o`, integer l)

Input : $0 < l \leq$ `o`.l
Result : i such that if `a`.$l = l - 1$ and `o` $\in$ desc(`a`), then `o` $\in$ desc(child(`a`)$[i]$)

1: $h \leftarrow 2^{l_{\max} - l}$ *[the* $(l_{\max} - l)$*th bits of the coordinates* `o`.x *describe the ancestor with level* l*]*
2: $i \leftarrow 0$
3: **for all** $0 \leq j < d$ **do**
4: $i \leftarrow i \mid ((\texttt{o}.x_j \ \& \ h) \ ? \ 2^j \ : \ 0)$ *["|" and "&" are bitwise OR and AND]*
5: **return** i

If we applied `Ancestor_id` to each octant in $\mathbf{A}$, we would get a monotonic sequence of integers, so if we search $\mathbf{A}$ with the key i and use `Ancestor_id` to test equality, the lowest matching index will give the first descendant of child(`a`)$[i]$ in $\mathbf{A}$. The split operation, however, is used repeatedly, both by `Search` and by the algorithm `Iterate` we will present in Section 5. To make this procedure as efficient as possible, we combine these searches into one algorithm `Split_array` (Algorithm 3.3), which is essentially an efficient binary search for a sorted list of keys.

4. Constructing ghost layers for unbalanced forests. As discussed in Section 2.4, there is no a-priori knowledge on any given process about what leaves might be in a neighboring process's partition. This knowledge, however, is necessary to determine the local neighborhoods of leaves that are adjacent to inter-process boundaries, which is crucial to many application-level algorithms. If a forest of octrees obeys a 2:1 balance condition, it is known that a leaf's neighbors in other partitions can differ by at most one refinement level. The previously presented algorithm `Ghost` [6, Algorithm 20] uses this fact to identify neighboring processes and communicate leaves between them. `Ghost` is short and effective, but not usable for an unbalanced forest. Here we present an algorithm for ghost layer construction that works for all forests. Its key component is a recursive algorithm that determines when a leaf's domain and a process's subdomain are adjacent to each other.

Algorithm 3.3: `Split_array` (octant array $\mathbf{A}$, octant $\mathtt{a}$)

Input : $\mathbf{A}$ is sorted; $\mathtt{a}$ is a strict ancestor of $\mathbf{A}[j]$ for each j, $\mathbf{A} \subseteq \text{desc}(\mathtt{a}) \backslash \{\mathtt{a}\}$.
Result : $\forall 0 \leq i < 2^d$, $\mathbf{H}[i]$ is a sorted array containing $\text{desc}(\text{child}(\mathtt{a})[i]) \cap \mathbf{A}$.

1: $\mathbf{k}[0] \leftarrow 0$ *[**invariant 1** $\forall i$: if $j \geq \mathbf{k}[i]$, ...]*
2: **for all** $1 \leq i \leq 2^d$ **do** $\mathbf{k}[i] \leftarrow |\mathbf{A}|$ *[... then* `Ancestor_id` $(\mathbf{A}[j], \mathtt{a}.l + 1) \geq i]$
3: **for** $i = 1$ **to** $2^d - 1$ **do**
4: $\quad m \leftarrow \mathbf{k}[i-1]$ *[**invariant 2:** if $j < m$, then* `Ancestor_id` $(\mathbf{A}[j], \mathtt{a}.l + 1) < i]$
5: $\quad$ **while** $m < \mathbf{k}[i]$ **do**
6: $\quad\quad n \leftarrow m + \lfloor (\mathbf{k}[i] - m)/2 \rfloor$ *[$\mathbf{k}[i-1] \leq m \leq n < \mathbf{k}[i]$]*
7: $\quad\quad c \leftarrow$ `Ancestor_id` $(\mathbf{A}[n],\ \mathtt{a}.l + 1)$ *[$\mathbf{A}[n] \in \text{desc}(\text{child}(\mathtt{a})[c])$]*
8: $\quad\quad$ **if** $c < i$ **then** *[$\mathbf{A}[n]$ is a descendant of a previous child]*
9: $\quad\quad\quad m \leftarrow n + 1$ *[increase lower bound to maintain invariant 2]*
10: $\quad\quad$ **else** *[$\mathbf{A}[n]$ is a descendant of the cth child, $c \geq i$]*
11: $\quad\quad\quad$ **for all** $i \leq j \leq c$ **do** $\mathbf{k}[j] \leftarrow n$ *[decrease $\mathbf{k}[j]$ to maintain invariant 1]*
12: **for all** $0 \leq i < 2^d$ **do** $\mathbf{H}[i] \leftarrow$ alias $\mathbf{A}[\mathbf{k}[i], \ldots, \mathbf{k}[i+1] - 1]$
13: **return** $\mathbf{H}$

4.1. Ghost layer construction using intersection tests. A leaf $\mathtt{o} \notin \mathcal{O}_\mathfrak{q}$ is in the *full ghost layer* for process $\mathfrak{q}$ if its boundary intersects the subdomain's closure, $\partial\text{Dom}(\mathtt{o}) \cap \overline{\Omega_\mathfrak{q}} \neq \emptyset$. This definition includes leaves whose intersection with $\overline{\Omega_\mathfrak{q}}$ is a single vertex. Some applications, such as discontinuous Galerkin finite element methods, only require a ghost layer to include leaves whose intersections with $\overline{\Omega_\mathfrak{q}}$ have codimension 1. The boundary set bound($\mathtt{o}$) (2.10) allows us to define a ghost layer parametrized by codimension. For $1 \leq k \leq d$, the $\mathfrak{p}$-*to*-$\mathfrak{q}$ *ghost layer* $\mathbf{G}^k_{\mathfrak{p}\to\mathfrak{q}}$ is a sorted array containing the subset of the leaves $\mathcal{O}_\mathfrak{p}$ whose boundaries intersect $\mathfrak{q}$'s subdomain at a point with codimension less than or equal to k,

$$\mathbf{G}^k_{\mathfrak{p}\to\mathfrak{q}} := \{\mathtt{o} \in \mathcal{O}_\mathfrak{p} : \exists\ \mathtt{c} \in \text{bound}(\mathtt{o}),\ \dim(\mathtt{c}) \geq d - k,\ \text{Dom}(\mathtt{c}) \cap \overline{\Omega_\mathfrak{q}} \neq \emptyset\}. \tag{4.1}$$

The *k-ghost layer* $\mathbf{G}^k_\mathfrak{p}$ for process $\mathfrak{p}$ is the sorted union of all $\mathfrak{q}$-to-$\mathfrak{p}$ ghost layers,

$$\mathbf{G}^k_\mathfrak{p} := \bigsqcup_{0\leq\mathfrak{q}<P,\ \mathfrak{q}\neq\mathfrak{p}} \mathbf{G}^k_{\mathfrak{q}\to\mathfrak{p}}. \tag{4.2}$$

To construct all $\mathbf{G}^k_{\mathfrak{p}\to\mathfrak{q}}$ according to (4.1), process $\mathfrak{p}$ would have to perform intersection tests between the boundary set of every leaf in $\mathcal{O}_\mathfrak{p}$ and every other process's subdomain. We can reduce the number of intersection tests by noting that if $\text{Dom}(\mathtt{c}) \cap \overline{\Omega_\mathfrak{q}} \neq \emptyset$, then by a corollary to Proposition 2.6, $\overline{\Omega_\mathfrak{q}}$ must overlap some octant $\mathtt{s}$ in the support set supp($\mathtt{c}$) that surrounds $\mathtt{c}$. Locating the first and last process subdomains that overlap Dom($\mathtt{s}$) for $\mathtt{s} \in \text{supp}(\mathtt{c})$ takes $O(\log P)$ time and typically reduces the number of intersection tests per point from $O(P)$ to $O(1)$. We give pseudocode for computing which $\mathfrak{p}$-to-$\mathfrak{q}$ ghost layers contain a leaf $\mathtt{o}$ in Algorithm 4.1.

Algorithm 4.1: `Add_ghost` (octant $\mathtt{o}$, integer k)

Input : octant $\mathtt{o} \in \mathcal{O}_\mathtt{p}$; $1 \le k \le d$.
Result : the set $\mathcal{Q}$ of processes $\mathtt{q}$ such that $\mathtt{o} \in \mathbf{G}^k_{\mathtt{p}\to\mathtt{q}}$ (4.1).

1: $\mathcal{Q} \leftarrow \emptyset$
2: **for all** $\mathtt{c} \in \text{bound}(\mathtt{o})$ **such that** $\dim(\mathtt{c}) \ge d-k$ **do**
3: **for all** $\mathtt{s} \in \text{supp}(\mathtt{c})\backslash\{\mathtt{o}\}$ **do**
4: $(\mathtt{f}_\mathtt{s}, \mathtt{l}_\mathtt{s}) \leftarrow \text{range}(\mathtt{s})$
5: $(\mathtt{q}_{\text{first}}, \mathtt{q}_{\text{last}}) \leftarrow (\text{locate}(\mathtt{f}_\mathtt{s}),\ \text{locate}(\mathtt{l}_\mathtt{s}))$ *[overlapping processes]*
6: **for all** $\mathtt{q}_{\text{first}} \le \mathtt{q} \le \mathtt{q}_{\text{last}}, \mathtt{q} \ne \mathtt{p}$ **do**
7: $(\mathtt{f}_\mathtt{q}, \mathtt{l}_\mathtt{q}) \leftarrow \text{range}(\mathtt{q})$ $[\ \overline{\Omega_\mathtt{q}} = \overline{\bigcup \text{Dom}([\mathtt{f}_\mathtt{q}, \mathtt{l}_\mathtt{q}])}\ ]$
8: $(\mathtt{f}, \mathtt{l}) \leftarrow (\max\{\mathtt{f}_\mathtt{s}, \mathtt{f}_\mathtt{q}\},\ \min\{\mathtt{l}_\mathtt{s}, \mathtt{l}_\mathtt{q}\})$ $[\ \overline{\bigcup \text{Dom}([\mathtt{f}, \mathtt{l}])} = \overline{\Omega_\mathtt{q}} \cap \overline{\text{Dom}(\mathtt{s})}\ ]$
9: **if** $\overline{\bigcup \text{Dom}([\mathtt{f}, \mathtt{l}])} \cap \text{Dom}(\mathtt{c}) \ne \emptyset$ **then** $\mathcal{Q} \leftarrow \mathcal{Q} \cup \{\mathtt{q}\}$
10: **return** $\mathcal{Q}$

4.2. Finding a range's boundaries recursively. The kernel of Algorithm 4.1 is the intersection test on line 9,

$$\left(\overline{\bigcup \text{Dom}([\mathtt{f}, \mathtt{l}])} \cap \text{Dom}(\mathtt{c}) = \emptyset?\right), \tag{4.3}$$

where $\mathtt{c}$ is a point, $[\mathtt{f}, \mathtt{l}]$ is the range between two atoms, and $\mathtt{f}$ and $\mathtt{l}$ are both descendants of an octant $\mathtt{s}$ in the support set $\text{supp}(\mathtt{c})$. We must specify how this intersection test is to be performed. Because $\mathtt{s} \in \text{supp}(\mathtt{c})$ implies $\mathtt{c} \in \text{bound}(\mathtt{s})$ (see Propositions 2.7 and 2.8), the point $\mathtt{c}$ must be equal to $(\mathtt{s}, b)$ for some boundary index $b \in \mathcal{B}$, so we can rephrase the test as $(\overline{\bigcup \text{Dom}([\mathtt{f}, \mathtt{l}])} \cap \text{Dom}((\mathtt{s}, b)) = \emptyset?)$. This test is a specific case of the problem of constructing the *range-boundary intersection* $\mathcal{B}_\cap(\mathtt{f}, \mathtt{l}, \mathtt{s})$, the set of all boundary indices b such that $\text{Dom}((\mathtt{s}, b))$ intersects the range,

$$\mathcal{B}_\cap(\mathtt{f}, \mathtt{l}, \mathtt{s}) := \{b \in \mathcal{B} : \overline{\bigcup \text{Dom}([\mathtt{f}, \mathtt{l}])} \cap \text{Dom}((\mathtt{s}, b)) \ne \emptyset\}. \tag{4.4}$$

If the range $[\mathtt{f}, \mathtt{l}]$ contains only descendants of some child of $\mathtt{s}$, say $\text{child}(\mathtt{s})[i]$, then the range-boundary intersection must be a subset of the *child-boundary intersection* $\mathcal{B}^i_\cap$, which is the subset of $\mathcal{B}$ corresponding to points in $\text{bound}(\mathtt{s})$ intersected by $\overline{\text{Dom}(\text{child}(\mathtt{s})[i])}$,

$$\mathcal{B}^i_\cap := \{b \in \mathcal{B} : \overline{\text{Dom}(\text{child}(\mathtt{s})[i])} \cap \text{Dom}((\mathtt{s}, b)) \ne \emptyset\}. \tag{4.5}$$

The child-boundary intersections $\{\mathcal{B}^i_\cap\}_{0 \le i < 2^d}$ (Figure 4.1, right) are the same for all (non-atom) octants. The following proposition, illustrated in Figure 4.1 (left), shows how the child-boundary intersection $\mathcal{B}^i_\cap$ relates $\mathcal{B}_\cap(\mathtt{f}, \mathtt{l}, \text{child}(\mathtt{s})[i])$ to $\mathcal{B}_\cap(\mathtt{f}, \mathtt{l}, \mathtt{s})$.

PROPOSITION 4.1 (Range-boundary intersection recursion). *If* $\mathtt{f}$ *and* $\mathtt{l}$ *are atoms,* $\mathtt{f} \le \mathtt{l}$*, and both are descendants of* $\text{child}(\mathtt{s})[i]$*, then*

$$(b \in \mathcal{B}_\cap(\mathtt{f}, \mathtt{l}, \mathtt{s})) \Leftrightarrow (b \in \mathcal{B}_\cap(\mathtt{f}, \mathtt{l}, \text{child}(\mathtt{s})[i]) \cap \mathcal{B}^i_\cap). \tag{4.6}$$

This result allows us to construct $\mathcal{B}_\cap(\mathtt{f}, \mathtt{l}, \mathtt{s})$ by partitioning $[\mathtt{f}, \mathtt{l}]$ into ranges for all of the overlapping children,

$$[\mathtt{f}, \mathtt{l}] = \bigsqcup_{i \in \mathcal{I}} [\mathtt{f}_i, \mathtt{l}_i], \quad \mathcal{I} := \{i : \exists \mathtt{a} \in \text{desc}(\text{child}(\mathtt{s})[i]),\ \mathtt{f} \le \mathtt{a} \le \mathtt{l}\}, \tag{4.7}$$

and constructing the range-boundary intersection for those children,

$$\mathcal{B}_\cap(\mathtt{f}, \mathtt{l}, \mathtt{s}) = \bigcup_{i \in \mathcal{I}} \mathcal{B}_\cap(\mathtt{f}_i, \mathtt{l}_i, \text{child}(\mathtt{s})[i]) \cap \mathcal{B}^i_\cap. \tag{4.8}$$

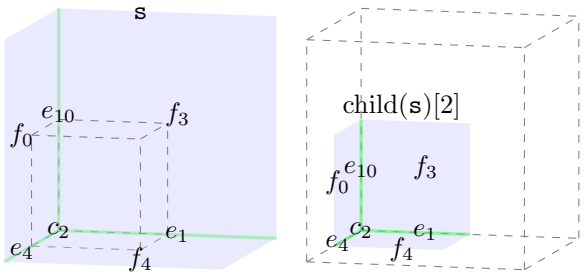

$\mathcal{B}^0_\cap$	$\{c_0, e_0, e_4, e_8, f_0, f_2, f_4\}$
$\mathcal{B}^1_\cap$	$\{c_1, e_0, e_5, e_9, f_1, f_2, f_4\}$
$\mathcal{B}^2_\cap$	$\{c_2, e_1, e_4, e_{10}, f_0, f_3, f_4\}$
$\mathcal{B}^3_\cap$	$\{c_3, e_1, e_5, e_{11}, f_1, f_3, f_4\}$
$\mathcal{B}^4_\cap$	$\{c_4, e_2, e_6, e_8, f_0, f_2, f_5\}$
$\mathcal{B}^5_\cap$	$\{c_5, e_2, e_7, e_9, f_1, f_2, f_5\}$
$\mathcal{B}^6_\cap$	$\{c_6, e_3, e_6, e_{10}, f_0, f_3, f_5\}$
$\mathcal{B}^7_\cap$	$\{c_7, e_3, e_7, e_{11}, f_1, f_3, f_5\}$

FIG. 4.1. *(left) An illustration of a specific instance of Proposition 4.1. If the range* $[\mathtt{f},\mathtt{l}]$ *contains only descendants of* $\mathrm{child}(\mathtt{s})[2]$*, then its domain intersects* $\mathrm{Dom}((\mathtt{s},b))$ *(left) if and only if it intersects* $\mathrm{Dom}((\mathrm{child}(\mathtt{s})[i],b))$ *(right) and* $b \in \mathcal{B}^2_\cap$*. (right) The child-boundary intersections are enumerated.*

This leads to the recursive algorithm `Find_range_boundaries` (Algorithm 4.2), which computes $\mathcal{B}_\cap(\mathtt{f},\mathtt{l},\mathtt{s}) \cap \mathcal{B}_{\text{query}}$ for a set $\mathcal{B}_{\text{query}} \subseteq \mathcal{B}$.

Algorithm 4.2: `Find_range_boundaries` (octants `f`, `l`, `s`, index set $\mathcal{B}_{\text{query}}$)

Input : `f` and `l` are atom descendants of `s`, $\mathtt{f} \le \mathtt{l}$; $\mathcal{B}_{\text{query}} \subseteq \mathcal{B}$.
Result : $\mathcal{B}_\cap(\mathtt{f},\mathtt{l},\mathtt{s}) \cap \mathcal{B}_{\text{query}}$ (4.4).

1: **if** $\mathcal{B}_{\text{query}} = \emptyset$ **or** $\mathtt{s}.l = l_{\max}$ **then return** $\mathcal{B}_{\text{query}}$
2: $j \leftarrow$ `Ancestor_id` $(\mathtt{f}, \mathtt{s}.l+1)$ *[index of first child whose range overlaps* $[\mathtt{f},\mathtt{l}]$*]*
3: $k \leftarrow$ `Ancestor_id` $(\mathtt{l}, \mathtt{s}.l+1)$ *[index of last child whose range overlaps* $[\mathtt{f},\mathtt{l}]$*]*
4: **if** $j = k$ **then return** `Find_range_boundaries` $(\mathtt{f},\mathtt{l},\mathrm{child}(\mathtt{s})[j], \mathcal{B}_{\text{query}} \cap \mathcal{B}^j_\cap)$
5: $\mathcal{B}_{\text{match}} \leftarrow \bigcup_{j<i<k} \mathcal{B}_{\text{query}} \cap \mathcal{B}^i_\cap$ *[boundary touched by wholly-covered children]*
6: $\mathcal{B}^j_{\text{match}} \leftarrow (\mathcal{B}_{\text{query}} \cap \mathcal{B}^j_\cap) \backslash \mathcal{B}_{\text{match}}$
7: $(\mathtt{f}_j, \mathtt{l}_j) \leftarrow \mathrm{range}(\mathrm{child}(\mathtt{s})[j])$ *[* $[\mathtt{f},\mathtt{l}] \cap [\mathtt{f}_j,\mathtt{l}_j] = [\mathtt{f},\mathtt{l}_j]$*: if* $\mathtt{f} \ne \mathtt{f}_j$*, recursion is needed]*
8: **if** $\mathtt{f} \ne \mathtt{f}_j$ **then** $\mathcal{B}^j_{\text{match}} \leftarrow$ `Find_range_boundaries` $(\mathtt{f},\mathtt{l}_j,\mathrm{child}(\mathtt{s})[j], \mathcal{B}^j_{\text{match}})$
9: $\mathcal{B}^k_{\text{match}} \leftarrow ((\mathcal{B}_{\text{query}} \cap \mathcal{B}^j_\cap) \backslash \mathcal{B}_{\text{match}}) \backslash B^j_{\text{match}}$
10: $(\mathtt{f}_k, \mathtt{l}_k) \leftarrow \mathrm{range}(\mathrm{child}(\mathtt{s})[k])$ *[* $[\mathtt{f},\mathtt{l}] \cap [\mathtt{f}_k,\mathtt{l}_k] = [\mathtt{f}_k,\mathtt{l}]$*: if* $\mathtt{l} \ne \mathtt{l}_k$*, recursion is needed]*
11: **if** $\mathtt{l} \ne \mathtt{l}_k$ **then** $\mathcal{B}^k_{\text{match}} \leftarrow$ `Find_range_boundaries` $(\mathtt{f}_k,\mathtt{l},\mathrm{child}(\mathtt{s})[k], \mathcal{B}^k_{\text{match}})$
12: **return** $(\mathcal{B}_{\text{match}} \cup \mathcal{B}^j_{\text{match}} \cup \mathcal{B}^k_{\text{match}})$

To compute the intersection test $(\overline{\bigcup \mathrm{Dom}([\mathtt{f},\mathtt{l}])} \cap \mathrm{Dom}((\mathtt{s},b)) = \emptyset?)$ in Algorithm 4.1, we choose $\mathcal{B}_{\text{query}} = \{b\}$ and use `Find_range_boundaries` to check whether $(\mathcal{B}_\cap(\mathtt{f},\mathtt{l},\mathtt{s}) \cap \mathcal{B}_{\text{query}} = \emptyset?)$. A proof of the correctness of Algorithm 4.2 is given in Appendix A. The recursive procedure is also illustrated in Figure 4.2.

4.3. Notes on implementation. Ghost layer construction in `Ghost` has a few optimizations not given in the pseudocode in Algorithm 4.1. Most leaves in $\mathcal{O}_\mathtt{p}$ do not touch the boundary of $\overline{\Omega_\mathtt{p}}$, and so cannot be in $\mathbf{G}^k_{\mathtt{p}\to\mathtt{q}}$ for any $\mathtt{q} \ne \mathtt{p}$. To avoid the intersection tests for these leaves, we first check to see if `o`'s 3×3 neighborhood (or "insulation layer" [24]) is owned by `p`: this can be accomplished with two comparisons, for the first and last atoms of the neighborhood, against the first-atoms array $\mathbf{f}$ (2.21). We also note that if `c` is a 0-point then $\overline{\Omega_\mathtt{q}}$ intersects $\mathrm{Dom}(\mathtt{c})$ if and only $\mathtt{q} = \mathrm{locate}(\mathtt{a})$ for some atom `a` in `c`'s atomic support set (2.12). Because this simpler test is available, we do not call `Find_range_boundaries` for 0-points.

If an instance of `Find_range_boundaries` calls two recursive copies of itself, all future instances will call only one recursive copy. We use this fact to take advantage

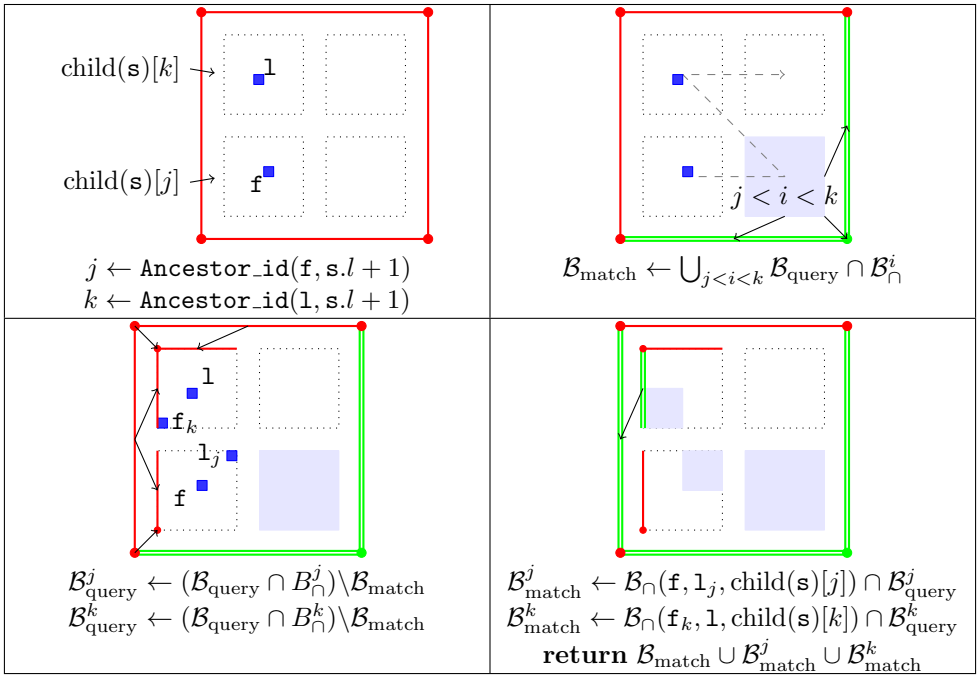

FIG. 4.2. *An illustration of* `Find_range_boundaries`*, listed in Algorithm 4.2. (top left) Solid red lines indicate the points in* bound(`s`) *indexed by* $\mathcal{B}_{\text{query}}$*; the children containing* `f` *and* `l` *are determined. (top right) The contribution to* $\mathcal{B}_{\cap}(\mathtt{f}, \mathtt{l}, \mathtt{s}) \cap \mathcal{B}_{\text{query}}$ *(double green lines) of children in the middle of the range is calculated; light blue indicates that this portion of the range* [`f`, `l`] *has been processed. (bottom left) The arguments for the recursive calls are constructed. (bottom right) The sets returned by the recursive calls are added to the return set.*

of tail-recursion optimization in our implementation. Because $|\mathcal{B}| < 32$ for $d = 2$ and $d = 3$, we can perform the set intersection, unions, and differences in Algorithm 4.2 by assigning each $b \in \mathcal{B}$ to a bit in an integer and performing bitwise operations.

5. A universal topology iterator. A forest is first of all a storage scheme for a mesh refinement topology. Applications use this topological information in ways that we do not wish to restrict or anticipate. We focus instead on designing an interface that conveys this information to applications in a complete and efficient manner, with the main goal of minimizing the points of contact between `p4est` on the one hand and the application on the other.

As we will see in our discussion of a specific node numbering algorithm in Section 6, some applications need to perform operations not just on leaves, but also on their boundary points. Our algorithm that facilitates this is called `Iterate`.

REMARK 5.1. The algorithm `Iterate` requires that the leaves in the micro layer $\mathcal{O}$ are 2:1 balanced. This is assumed for the remainder of this section and Section 6. This assumption is not very limiting: most applications that need topological information (e.g., finite element or fast multipole calculations) require 2:1 balance, either for numerical reasons or to avoid the complexity of handling general adjacencies. On the other hand, extending the algorithm to larger refinement ratios when the need arises appears to be a practical option since this case is covered by the recursion as well.

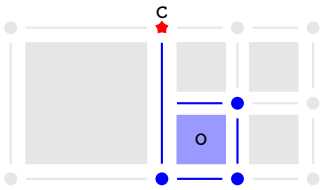

FIG. 5.1. *Suppose process* $\mathtt{p}$ *owns only octant* $\mathtt{o}$ *in this two-dimensional illustration.* $\mathcal{P}_\Omega$ *is the set of all points shown: note that because some points in* $\mathrm{clos}(\mathtt{o})$ *are hanging, they are not included. The set* $\mathcal{P}_\mathtt{p}$ *of points that overlap* $\overline{\Omega_p}$ *is shown in blue. The* 0*-point* $\mathtt{c}$ *shown as a red star is not in* $\mathcal{P}_\mathtt{p}$*, but is in its closure,* $\overline{\mathcal{P}_\mathtt{p}}$*.*

5.1. Definitions. The algorithm `Iterate` is distributed and communication-free (assuming that the ghost layer $\mathbf{G}^d_\mathtt{p}$ (4.2) has already been constructed): on process $\mathtt{p}$, it takes a user-supplied callback and executes it once for every leaf and leaf-boundary point $\mathtt{c}$ that is relevant to $\mathcal{O}_\mathtt{p}$, supplying information about the neighborhood around $\mathtt{c}$. We define exactly what this means here.

The union of all leaves with their closure sets, $\bigcup \mathrm{clos}(\mathcal{O})$, defines a covering of Ω, $\overline{\Omega} = \bigcup \mathrm{Dom}(\bigcup \mathrm{clos}(\mathcal{O}))$. This covering may not be a partition, because $\bigcup \mathrm{clos}(\mathcal{O})$ may contain *hanging* points: n-points of dimension $n < d$ that are in the child partition sets (2.7) of other points in $\bigcup \mathrm{clos}(\mathcal{O})$. We can define a partition by removing these hanging points. The *global partition* $\mathcal{P}_\Omega$ is

$$\mathcal{P}_\Omega := \bigcup \mathrm{clos}(\mathcal{O}) \backslash \{\mathtt{c} : \exists\ \mathtt{e} \in \bigcup \mathrm{clos}(\mathcal{O}),\ \mathtt{c} \in \mathrm{part}(\mathtt{e})\}. \tag{5.1}$$

If there is just one process, the function `Iterate` executes a user-supplied callback function for every point $\mathtt{c} \in \mathcal{P}_\Omega$. For a distributed forest, `Iterate` as called by process $\mathtt{p}$ executes the callback function only for the subset of $\mathcal{P}_\Omega$ that is relevant to $\mathcal{O}_\mathtt{p}$. In the `p4est` implementation, we allow for two definitions of what is relevant. The first is the *locally relevant partition*, which is the subset $\mathcal{P}_\mathtt{p} \subseteq \mathcal{P}_\Omega$ that overlaps $\overline{\Omega_\mathtt{p}}$,

$$\mathcal{P}_\mathtt{p} := \{\mathtt{c} \in \mathcal{P}_\Omega : \exists\ \mathtt{o} \in \mathcal{O}_\mathtt{p},\ \mathrm{Dom}(\mathtt{c}) \cap \overline{\mathrm{Dom}(\mathtt{o})} \neq \emptyset\}. \tag{5.2}$$

One potential problem with $\mathcal{P}_\mathtt{p}$ is that, because of hanging points, it may not be closed: if $\mathtt{c} \in \mathcal{P}_\mathtt{p}$, there may be $\mathtt{e} \in \mathrm{clos}(\mathtt{c})$ such that $\mathtt{e} \notin \mathcal{P}_\mathtt{p}$. As we will show in Section 6, closedness is necessary for some applications, so we also define the *closed locally relevant partition* $\overline{\mathcal{P}_\mathtt{p}}$,

$$\overline{\mathcal{P}_\mathtt{p}} := \bigcup \{\mathrm{clos}(\mathtt{e}) :\ \mathtt{e} \in \mathcal{P}_\mathtt{p}\}. \tag{5.3}$$

The sets we have defined thus far—$\mathcal{P}_\Omega$, $\mathcal{P}_\mathtt{p}$, and $\overline{\mathcal{P}_\mathtt{p}}$—are illustrated in Figure 5.1.

If `Iterate` only supplied the callback with each relevant point $\mathtt{c}$ in isolation, its utility would be limited, because it would say nothing about the neighborhood around $\mathtt{c}$. We call the neighborhood of adjacent leaves the *leaf support set* $\mathrm{leaf\,supp}(\mathtt{c})$,

$$\mathrm{leaf\,supp}(\mathtt{c}) := \{\mathtt{o} \in \mathcal{O} : \overline{\mathrm{Dom}(\mathtt{o})} \cap \mathrm{Dom}(\mathtt{c}) \neq \emptyset\}. \tag{5.4}$$

Note that the leaf support set $\mathrm{leaf\,supp}(\mathtt{c})$ may differ from the support set $\mathrm{supp}(\mathtt{c})$ (2.11), which is independent of the leaves in the micro layer $\mathcal{O}$. Because process $\mathtt{p}$ does not have access to all leaves in $\mathcal{O}$, it can only compute the subset of the leaf support

set that is contained in the local leaves and in the full ghost layer $\mathbf{G}_\mathtt{p}^d$ (4.2), which we call the *local leaf support set* $\operatorname{leaf supp}_\mathtt{p}(\mathtt{c})$,

$$\operatorname{leaf supp}_\mathtt{p}(\mathtt{c}) := \operatorname{leaf supp}(\mathtt{c}) \cap (\mathcal{O}_\mathtt{p} \cup \mathbf{G}_\mathtt{p}^d). \tag{5.5}$$

PROPOSITION 5.2. $\operatorname{leaf supp}_\mathtt{p}(\mathtt{c}) = \operatorname{leaf supp}(\mathtt{c})$ *if and only if* $\mathtt{c} \in \mathcal{P}_\mathtt{p}$.

The local leaf support set, though it may not contain all of the leaf support set, is what `Iterate` supplies to the user-supplied callback to describe the neighborhood around `c`. The local leaf support set can be used to determine if $\mathtt{c} \in \mathcal{P}_\mathtt{p}$ or $\mathtt{c} \in \overline{\mathcal{P}_\mathtt{p}}$, using a function `Is_relevant` (Algorithm 5.1).

Algorithm 5.1: `Is_relevant` (point `c`, octant set $\operatorname{leaf supp}_\mathtt{p}(\mathtt{c})$)

Input : $\operatorname{leaf supp}_\mathtt{p}(\mathtt{c})$ is the local leaf support set of `c` (5.5).
Result : true if and only if `c` is in the relevant set ($\mathcal{P}_\mathtt{p}$ or $\overline{\mathcal{P}_\mathtt{p}}$).

```
1: for all s ∈ leaf supp_p(c) do
2:     if s ∈ O_p then return true
3:     else                                  [this else-statement is only used if P̄_p is relevant ]
4:         for all e ∈ bound(s) such that c ∈ bound(e) do
5:             if Dom(e) ∩ Ω̄_p ≠ ∅ then return true      [intersection test from Section 4.2 ]
6: return false
```

For each octant $\mathtt{o} \in \operatorname{leaf supp}_\mathtt{p}(\mathtt{c})$, the `p4est` implementation of `Iterate` supplements the octant data fields $\mathtt{o}.l$, $\mathtt{o}.x$, and $\mathtt{o}.t$ with additional data passed to the callback function. We supply a boolean identifying whether $\mathtt{o} \in \mathcal{O}_\mathtt{p}$, so no searching is necessary to determine if `o` is local or a ghost. We also supply the index of `o` within either $\mathbf{O}_\mathtt{p}^t$ for $t = \mathtt{o}.t$ (which is easily converted to j such that $\mathcal{O}_\mathtt{p}[j] = \mathtt{o}$) or within the ghost layer $\mathbf{G}_\mathtt{p}^d$ (4.2). Keeping track of this information does not change the computational complexity of `Iterate`, but introduces additional bookkeeping that we will omit from our presentation of the algorithm.

5.2. Iterating in the interior of a point. A simple implementation of `Iterate` might take each leaf $\mathtt{o} \in \mathcal{O}_\mathtt{p}$ in turn and, for each $\mathtt{c} \in \operatorname{bound}(\mathtt{o})$, compute $\operatorname{leaf supp}_\mathtt{p}(\mathtt{c})$ by searching through $\mathcal{O}_\mathtt{p}$ and $\mathbf{G}_\mathtt{p}^d$ to find `o`'s neighbors that are adjacent to `c`. A bounded number of binary searches would be performed per leaf, so the total iteration time would be $O(N_\mathtt{p} \log N_\mathtt{p})$. This is the strategy used by the `Nodes` algorithm in `p4est` [6, Algorithm 21] and by other octree libraries [27]. We note two problems with this approach. The first is the large number of independent searches that are performed. The second is that this approach needs some way of ensuring that the callback is executed for each relevant point only once, such as storing the set of points for which the callback has executed in a hash table.

Instead, the implementation of `Iterate` that we present proceeds recursively. We take as inputs to the recursive procedure a point `c` and a set of arrays $\mathbf{S}$, where $\mathbf{S}[i]$ contains all leaves that are descendants of the support set octant $\operatorname{supp}(\mathtt{c})[i]$. If `c` is in the global partition $\mathcal{P}_\Omega$ and is in the relevant set ($\mathcal{P}_\mathtt{p}$ or $\overline{\mathcal{P}_\mathtt{p}}$), then the octants in $\operatorname{leaf supp}_\mathtt{p}(\mathtt{c})$ can be found in the $\mathbf{S}$ arrays and the callback function can be executed. Otherwise, the points of the global partition $\mathcal{P}_\Omega$ that are descendants of `c` can be divided between the points in the child partition set $\operatorname{part}(\mathtt{c})$ (2.7). Each $\mathtt{e} \in \operatorname{part}(\mathtt{c})$ takes the place of `c` in a call to the recursive procedure: to compute the new $\mathbf{S}$ arrays for `e`, we use the function `Split_array` (described in Section 3.2) on the original arrays $\mathbf{S}$. This is spelled out in `Iterate_interior` (Algorithm 5.2).

We provide some figures to illustrate the recursion in `Iterate_interior`: Figure 5.2 shows the cases when $\dim(\mathtt{c}) = d$ and $0 < \dim(\mathtt{c}) < d$ and Figure 5.3 shows

Algorithm 5.2: `Iterate_interior` (point `c`, octant arrays $\mathbf{S}$, `callback`)

Input : $\mathbf{S}[i]$ is the sorted array of all leaves $\mathtt{o} \in \mathcal{O}_\mathtt{p} \cup \mathbf{G}^d_\mathtt{p}$ such that $\mathtt{o} \in \mathrm{desc}(\mathrm{supp}(\mathtt{c})[i])$.
Result : if $\mathtt{c} \in \mathcal{P}_\mathtt{p}$ (or $\overline{\mathcal{P}_\mathtt{p}}$), then $\mathrm{leaf\,supp}_\mathtt{p}(\mathtt{c})$ (5.5) is computed and passed to `callback`; otherwise, `callback` is called for each $\mathtt{e} \in \mathcal{P}_\mathtt{p}$ (or $\overline{\mathcal{P}_\mathtt{p}}$) such that $\mathrm{Dom}(\mathtt{e}) \subset \mathrm{Dom}(\mathtt{c})$.

1: **if** $\bigcup \mathbf{S} \cap \mathcal{O}_\mathtt{p} = \emptyset$ **then return** *[stop if there are no local leaves]*
2: octant set $\mathcal{L} \leftarrow \emptyset$ *[if $\mathtt{c} \in \mathcal{P}_\Omega$, then $\mathcal{L}$ will equal $\mathrm{leaf\,supp}_\mathtt{p}(\mathtt{c})$]*
3: boolean stop $\leftarrow$ **false** *[stop will be true if $\mathtt{c} \in \mathcal{P}_\Omega$]*
4: **if** $\dim(\mathtt{c}) > 0$ **then** *[see Figure 5.2]*
5: | **for all** $0 \le i < |\mathrm{supp}(\mathtt{c})|$ **do**
6: | | $\mathtt{s} \leftarrow \mathrm{supp}(\mathtt{c})[i]$
7: | | **if** $\mathbf{S}[i] = \{\mathtt{s}\}$ **then** *[if $\mathtt{s}$ is a leaf, ...]*
8: | | | stop $\leftarrow$ **true** *[then $\mathtt{c} \in \mathcal{P}_\Omega$, ...]*
9: | | | $\mathcal{L} \leftarrow \mathcal{L} \cup \{\mathtt{s}\}$ *[and $\mathtt{s} \in \mathrm{leaf\,supp}(\mathtt{c})$]*
10: | | **else**
11: | | | $\mathbf{H}_i \leftarrow$ `Split_array`$(\mathbf{S}[i], \mathtt{s})$ *[$O(\log|\mathbf{S}[i]|)$ (see Section 3.2)]*
12: | | | $\mathbf{h}_i \leftarrow \mathrm{child}(\mathtt{s})$ *[if $\mathtt{c} \in \mathcal{P}_\Omega$, then by the 2:1 condition, ...]*
13: | | | $b \leftarrow b$ such that $\mathtt{c} = (\mathtt{s}, b)$ *[children next to $(\mathtt{s}, b) = \mathtt{c}$ are in $\mathrm{leaf\,supp}(\mathtt{c})$]*
14: | | | $\mathcal{L} \leftarrow \mathcal{L} \cup \{\mathbf{h}_i[j] : b \in \mathcal{B}^j_\cap\}$ *[$\mathcal{B}^j_\cap$ are child-boundary intersection sets (4.5)]*
15: **else** *[a 0-point, see Figure 5.3]*
16: | stop $\leftarrow$ **true** *[anytime we find a 0-point between leaves, it is in $\mathcal{P}_\Omega$.]*
17: | **for** $0 \le i < |\mathrm{supp}(\mathtt{c})|$ **do** *[find leaves surrounding `c`: use Proposition 2.8]*
18: | | $\mathcal{L} \leftarrow \mathcal{L} \cup \{\mathtt{o} \in \mathbf{S}[i] : \mathrm{atom\,supp}(\mathtt{c})[i] \in \mathrm{desc}(\mathtt{o})\}$ *[requires $O(\log|\mathbf{S}[i]|)$ search]*
19: **if** stop **then**
20: | **if** `Is_relevant`$(\mathtt{c}, \mathcal{L})$ **then** `callback`$(\mathtt{c}, \mathcal{L})$
21: **else**
22: | **for all** $\mathtt{e} \in \mathrm{part}(\mathtt{c})$ **do** *[set up recursion for each point in child partition set (2.7)]*
23: | | **for all** $0 \le i < |\mathrm{supp}(\mathtt{e})|$ **do** *[find descendants of support set octants]*
24: | | | $\mathbf{S}_\mathtt{e}[i] \leftarrow \mathbf{H}_j[k]$ such that $\mathbf{h}_j[k] = \mathrm{supp}(\mathtt{e})[i]$ *[subarrays created on line 11]*
25: | `Iterate_interior`$(\mathtt{e}, \mathbf{S}_\mathtt{e}, \mathtt{callback})$

the case when $\dim(\mathtt{c}) = 0$. The correctness of Algorithm 5.2 is proved in Appendix B.

REMARK 5.3. An instance of `Iterate_interior` may call multiple recursive copies of itself: one for each point in the child partition set $\mathrm{part}(\mathtt{c})$ (see the loop starting on line 22). We have not yet specified an order for these recursive calls. In our implementation, we have chosen to order these calls by decreasing point dimension. This guarantees that, if $\mathtt{e} \in \mathrm{bound}(\mathtt{c})$, then the callback is executed for `c` before it is executed for `e`. We take advantage of this order in designing a node-numbering algorithm in Section 6.

5.3. Iterating on a forest. To iterate on the complete forest, each process must call `Iterate_interior` for the closure set of the root of every tree. This is listed in `Iterate` (Algorithm 5.3). Asymptotic analysis of the performance of `Iterate` is given in Appendix C: it shows that, in general, `Iterate` executes in $\mathcal{O}(((\max_{\mathtt{o} \in \mathcal{O}} \mathtt{o}.l) + N_\mathtt{p}) \log N_\mathtt{p})$ time, but if the refinement pattern of the octrees in the forest is uniform or nearly so, then it executes in $\mathcal{O}(\log P + N_\mathtt{p})$ time.

5.4. Implementation. The implementation of `Iterate` in `p4est` has some differences from the presented algorithm to optimize performance. `Iterate_interior` is implemented in while-loop form to keep the stack from growing: all space needed for recursion (which is $O(l_{\max})$) is pre-allocated on the heap. We noticed in early tests that `Split_array` can be called with the same arguments multiple times during a call to `Iterate`. To avoid some of this recomputation, we keep an $O(l_{\max})$ fixed-size

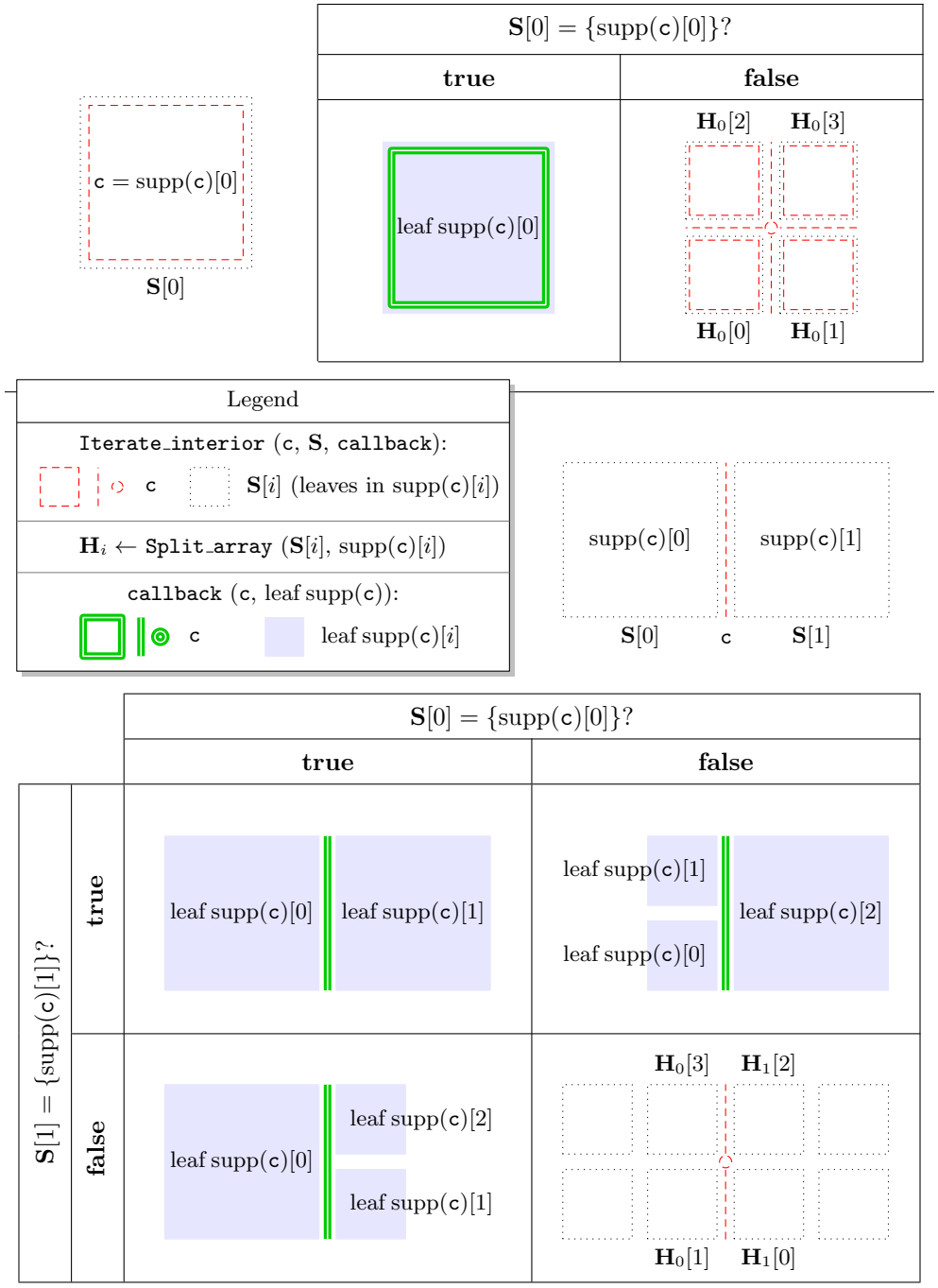

FIG. 5.2. *Illustrations of* `Iterate_interior` *for* $\dim(\mathtt{c}) = d$ *(top) and* $0 < \dim(\mathtt{c}) < d$ *(bottom). Dashed red lines indicates the argument point* `c` *of* `Iterate_interior`*. The dotted squares indicate the arrays* $\mathbf{S}[i]$ *of leaves in* $\mathcal{O}$ *that are descendants of* $\mathrm{supp}(\mathtt{c})[i]$*. If* $\mathrm{supp}(\mathtt{c})[i]$ *is a leaf (which is determined by testing whether* $\mathbf{S}[i] = \{\mathrm{supp}(\mathtt{c})[i]\}$*), then it is in* $\mathrm{leaf}\,\mathrm{supp}(\mathtt{c})$*, which is shown with the solid color blue; otherwise,* $\mathbf{S}[i]$ *is split using* `Split_array`*. If a leaf has been found, the user-supplied callback function is executed, which we indicate with double color green lines; otherwise,* `Iterate_interior` *is called for each point in the child partition set* $\mathrm{part}(\mathtt{c})$*: the support sets for these points are found in the children of the octants in* $\mathrm{supp}(\mathtt{c})$*, and the arrays of leaves contained in them are found in the sets created by* `Split_array`*.*

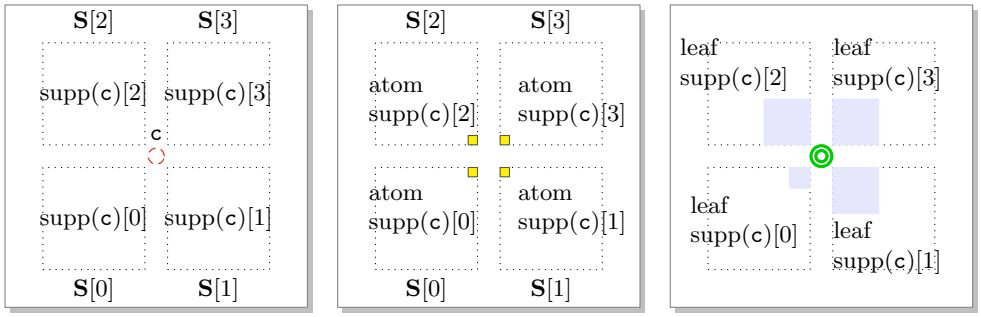

FIG. 5.3. *An illustration of* `Iterate_interior` *when* $\dim(\mathtt{c}) = 0$*, using the same color conventions as Figure 5.2. The arguments of* `Iterate_interior` *are in the left panel. The small squares (middle panel) indicate octants in* $\operatorname{atom}\operatorname{supp}(\mathtt{c})$*: these must be descendants of the leaves in* $\operatorname{leaf}\operatorname{supp}(\mathtt{c})$*, so we use* $\operatorname{atom}\operatorname{supp}(\mathtt{c})[i]$ *as a key to search for* $\operatorname{leaf}\operatorname{supp}(\mathtt{c})[i]$ *in* $\mathbf{S}[i]$*. Once* $\operatorname{leaf}\operatorname{supp}(\mathtt{c})$ *is found, the callback is executed (right panel).*

Algorithm 5.3: `Iterate` (`callback`, octant array $\mathbf{G}_{\mathtt{p}}^d$)

Input : $\mathbf{G}_{\mathtt{p}}^d$ is the full ghost layer (4.2).
Result : if $\mathtt{c} \in \mathcal{P}_{\mathtt{p}}$ (or $\overline{\mathcal{P}_{\mathtt{p}}}$), $\operatorname{leaf}\operatorname{supp}_{\mathtt{p}}(\mathtt{c})$ is computed and passed to `callback`.

1: **for all** $0 \le t < K$ **do**
2: $\quad \mathbf{G}^t \leftarrow \mathbf{G}_{\mathtt{p}}^d \cap \mathcal{O}^t$ *[subset of the ghost layer for tree t* $(O(\log|\mathbf{G}_{\mathtt{p}}^d|))$ *]*
3: $\quad \mathbf{S}^t \leftarrow \mathbf{O}_{\mathtt{p}}^t \cup \mathbf{G}^t$ *[* $\mathbf{O}_{\mathtt{p}}^t$ *and* $\mathbf{G}^t$ *are already ordered: no sorting is necessary]*
4: **for all** $\mathtt{c} \in \bigcup_{0\le t<K} \operatorname{clos}(\operatorname{root}(t))$ **do**
5: $\quad$ **for all** $0 \le i < |\operatorname{supp}(\mathtt{c})|$ **do**
6: $\quad\quad t \leftarrow \operatorname{supp}(\mathtt{c})[i].t$ *[Each* $\operatorname{supp}(\mathtt{c})[i]$ *is the root of an octree]*
7: $\quad\quad \mathbf{U}[i] \leftarrow \mathbf{S}^t$
8: $\quad$ `Iterate_interior` (`c`, **U**, `callback`)

cache of the array aliases produced by `Split_array`. We allow the user to specify a separate callback function for each dimension, so that extra recursion can be avoided. If, for example, the callback only needs to be executed for faces, then an instance of `Interate_interior` operating on `c` will only call a recursive copy for $\mathtt{e} \in \operatorname{part}(\mathtt{c})$ if $\dim(\mathtt{e}) \ge d - 1$.

6. A use case for the iterator: higher-order nodal basis construction. Thus far, we have developed algorithms for distributed forests with no special regard for numerical applications. In this section, we use our framework to perform a classic but complex task necessary for finite element computations, namely the globally unique numbering of degrees of freedom for a continuous finite element space over hanging-node meshes. We call it `Lnodes` in reference to (Gauß-)Lobatto nodes, which means that some nodes are located on element boundaries and are thus shared between multiple elements and/or processes, which presents some interesting challenges.

Hanging-node data structures have been discussed as early as 1980 [23] and adapted effectively for higher-order spectral element computations [11, 25]. Special-purpose data structures and interface routines have been defined for many discretization types built on top of octrees, including piecewise linear tensor-product elements [1, 5] and discontinuous spectral elements [29]. The `deal.II` finite element software [3] uses yet another mesh interface [2]. In our presentation of `Lnodes`, we hope to show that the `Iterate` approach is sufficiently generic that it could be used to efficiently construct

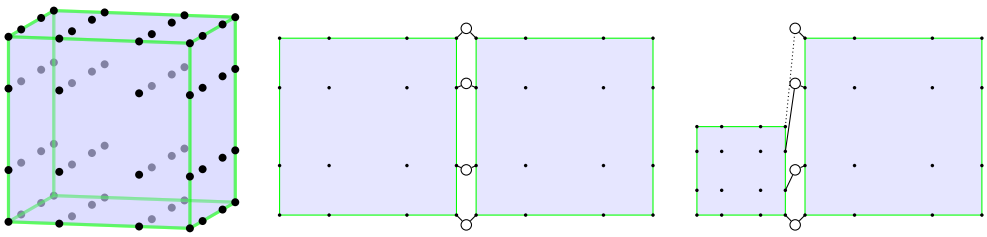

FIG. 6.1. *(left) Q^n-nodes for $n = 3$, with one node at each corner, $n - 1$ nodes on (the interior of) each edge, $(n - 1)^2$ nodes on each face, and $(n - 1)^3$ nodes in each element. (middle, right) For both conformal and non-conformal interfaces, each element node corresponds to exactly one global node. (right) At non-conformal interfaces, an element may reference a global node remotely, as the small element references the top node.*

any of these data structures.

6.1. Concepts. In a hexahedral n-order nodal finite element, the Lagrangian basis functions and the degrees of freedom are associated with $(n + 1)^3$ *Q^n-nodes* located on a tensor grid of locations in the element. There is one node at each corner, $(n - 1)$ nodes in the interior of each edge, $(n - 1)^2$ nodes in the interior of each face, and $(n - 1)^3$ nodes in the interior of the element, as in Figure 6.1 (left). If we endow each leaf in a forest of octrees with Q^n-nodes, we get $N \times (n + 1)^3$ *element nodes*. Q^n-nodes are numbered lexicographically, and element-local nodes are then numbered to match the order of their associated leaves. The basis functions associated with the element nodes span a discontinuous approximation space.

We want to create a nodal basis for a C^0-conformal approximation space on Ω such that the restriction of the space to any leaf is spanned by the Q^n-nodes' basis functions. The nodes for the continuous basis functions are called *global nodes*. Each of the element nodes in the interior of a leaf can be associated with a unique global node, but on the boundary of a leaf, element nodes from multiple leaves may occupy the same location: in this case, the two element nodes are associated with the same global node, as in Figure 6.1 (middle). For non-conformal interfaces, the element nodes of the smaller leaves are not at the same locations as those of the larger leaf, but they cannot introduce new degrees of freedom, because every function in the space, when restricted to the non-conformal interface, must be representable using the larger leaf's basis functions. Conceptually, we can place the global nodes at the locations of the larger leaf's nodes and associate each element node from the smaller leaves with a single global node, as shown in Figure 6.1 (right). In reality, the value of a function at an element node on a non-conformal interface must be interpolated from the values at multiple global nodes, but the conceptual one-to-one association between a leaf's element nodes and global nodes is sufficient, in that it identifies all global nodes whose basis functions are supported on that leaf.

It is important to note that an element node of a leaf o may reference a global node that is contained in the domain of a point c that is outside the closure $\mathrm{Dom}(\mathsf{o})$, and that o is therefore not in the set of adjacent leaves $\mathrm{leaf\,supp}(\mathsf{c})$ defined in (5.4). In this situation, we say that o *remotely references* the global nodes in c. Formally, a leaf o remotely references a point c in the global partition set $\mathcal{P}_\Omega$ if

$$\mathsf{c} \notin \mathrm{leaf\,supp}(\mathsf{c}) \text{ and } \exists \mathsf{e} \text{ such that } \mathsf{o} \in \mathrm{leaf\,supp}(\mathsf{e}) \text{ and } \mathsf{c} \in \mathrm{bound}(\mathsf{e}). \tag{6.1}$$

This relationship is also shown in Figure 6.1 (right). From this definition, we can see

that the global nodes referenced by leaves in $\mathcal{O}_\mathtt{p}$ will be contained in the closed locally relevant partition $\overline{\mathcal{P}_\mathtt{p}}$ (5.3). We note that a point $\mathtt{c}$ can be remotely referenced only if $\dim(\mathtt{c}) < d-1$.

6.2. Data structures. On process $\mathtt{p}$, we can represent the global nodes using an array $\mathbf{N}_\mathtt{p}$ and the element nodes using a double array $\mathbf{E}_\mathtt{p}$, where $\mathbf{E}_\mathtt{p}[j][k]$ maps the kth element node of $\mathcal{O}_\mathtt{p}[j]$ to its global node in $\mathbf{N}_\mathtt{p}$. $\mathbf{N}_\mathtt{p}$ and $\mathbf{E}_\mathtt{p}$ only reference locally relevant global nodes and thus implement fully distributed parallelism.

In presenting the `Lnodes` algorithm, we consider a global node $\mathtt{g}$ to have the following data fields:

- $\mathtt{g}.i$: the globally unique *index* of this node,
- $\mathtt{g}.\mathtt{p}$: the *process* that owns $\mathtt{g}$ for the purposes of scatter/gather communication of node values,
- $\mathtt{g}.\mathcal{S}_{\text{share}}$: the *sharer set* of all processes that reference this node.

We include the sharer set $\mathcal{S}_{\text{share}}$ so that, in addition to the scatter/gather communication paradigm, the global nodes can also be used in the share-all paradigm, wherein any process that shares a node can send information about that node to all other processes that share that node.[5] If each process generates new information about a node, the former paradigm requires two rounds of communication for information to disseminate, one gather and one scatter, while the latter requires one round, but with an increased number of messages. Each paradigm can be faster than the other, depending on communication latency, bandwidth, and other factors. We tend to place the highest weight on latency, hence our added support for share-all.

REMARK 6.1. Most applications do not require higher-order finite element nodes, but the `Lnodes` data structure can be used in much more general settings. In particular, the `Lnodes` data structures for $n = 2$ assign one unique global index to every point in $\overline{\mathcal{P}_\mathtt{p}}$, and a map from each leaf to the points in its closure. If one symmetrizes these mappings, i.e., if one saves the leaf support sets $\operatorname{leaf}\operatorname{supp}_\mathtt{p}(\mathtt{c})$ for $\mathtt{c} \in \overline{\mathcal{P}_\mathtt{p}}$ generated by `Iterate`, then one has essentially converted the forest-of-octrees data structures into a graph-based unstructured mesh format with $O(1)$ local topology traversal. This format is typical of generic finite element libraries. `Lnodes` can therefore serve as the initial step in converting a forest of octrees into the format of an external library, with the remaining steps requiring little or no communication between processes.

6.3. Assigning global nodes. We want global nodes to be numbered independently of the number of processes P and the partition of the leaves. For this reason, it is useful for each global node to be owned by one leaf, because a partition-independent order is then induced by combining lexicographic ordering of element nodes with the total octant order (see Algorithm 2.1). This computation is shown in Algorithm 6.1, which assumes that we have already determined which leaf $\mathcal{O}_\mathtt{p}[j]$ owns each global node $\mathtt{g}$, and temporarily stored that leaf's index in the global node's $\mathtt{g}.i$ field.

We need a policy for assigning the ownership of nodes to leaves. We assign point $\mathtt{c} \in \mathcal{P}_\Omega$ and its nodes to the first leaf $\mathtt{o}$ in $\operatorname{leaf}\operatorname{supp}(\mathtt{c})$,

$$\operatorname{owner}(\mathtt{c}) := \min \operatorname{leaf}\operatorname{supp}(\mathtt{c}). \tag{6.2}$$

In the next subsection, we will show how this assignment policy allows for the global nodes to be constructed without any more communication between processes than the communication in `Global_numbering`.

[5] In `p4est`, the implementation differs: rather than the per-node lists $\mathtt{g}.\mathcal{S}_{\text{share}}$, we store lists of nodes that are shared by each process, which is a more useful layout for filling communication buffers.

Algorithm 6.1: `Global_numbering` (global node array $\mathbf{N}_\mathtt{p}$, double array $\mathbf{E}_\mathtt{p}$)

Input : $\forall \mathtt{g} \in \mathbf{N}_\mathtt{p}$, $\mathtt{g}.\mathtt{p} = \mathtt{q}$ such that the leaf that owns $\mathtt{g}$ is in $\mathcal{O}_\mathtt{q}$; if $\mathtt{g}.\mathtt{p} = \mathtt{p}$, then $\mathtt{g}.\mathcal{S}_{\text{share}}$ is correct and $\mathtt{g}.i = j$ is (temporarily abused as) the index of the leaf that owns $\mathtt{g}$, $\mathcal{O}_\mathtt{p}[j]$.

Result : correct global node data for all $\mathtt{g} \in \mathbf{N}_\mathtt{p}$.

```
1:  integer array M[|N_p|]                          [temporarily stores the local indices of global nodes]
2:  m ← 0                                           [the number of global nodes owned by p]
3:  for j = 0 to |O_p| − 1 do
4:      for l = 0 to (n + 1)^d − 1 do
5:          k ← E_p[j][l]        [index in N_p of the global node referenced by this element node]
6:          if N_p[k].p = p and N_p[k].i = j then
7:              M[k] ← m                                [g's index among the locally owned nodes]
8:              m ← m + 1
9:  t ← Prefix_sums(Allgather(m))                   [ t[q] is the offset to the first node owned by q]
10: for all 0 ≤ k < |N_p| do
11:     g ← N_p[k]
12:     if g.p = p then
13:         g.i ← M[k] + t[p]                                [all fields of g are now complete]
14:         send g to each q ∈ g.S_share      [in practice, grouped into one message per process]
15:     else
16:         receive updated g from g.p
```

6.4. The `Lnodes` algorithm. The `Lnodes` algorithm (Algorithm 6.2) creates the global nodes and element nodes by iterating a callback `Lnodes_callback` over all points in the closed locally relevant partition $\overline{\mathcal{P}_\mathtt{p}}$, which sets up a call to `Global_numbering` (Algorithm 6.1).

Algorithm 6.2: `Lnodes` (integer n, ghost layer $\mathbf{G}_\mathtt{p}^d$)

Input : $n > 0$, the order of the nodes; the full ghost layer $\mathbf{G}_\mathtt{p}^d$ (4.2).

Result : a double array $\mathbf{E}_\mathtt{p}$ of $N_\mathtt{p} \times (n+1)^d$ indices that maps element nodes to global nodes; an array $\mathbf{N}_\mathtt{p}$ of global nodes.

```
1: global node array N_p ← ∅
2: integer double array E_p[|O_p|][(n + 1)^d]
3: Iterate (Lnodes_callback, G_p^d)                          [initialize N_p, E_p]
4: Global_numbering (N_p, E_p)                               [finalize N_p]
```

Given the assumptions of `Global_numbering`, `Lnodes_callback` has to accomplish the following for each global node $\mathtt{g}$ located at a point $\mathtt{c} \in \overline{\mathcal{P}_\mathtt{p}}$ visited by `Iterate`:

1. determine the process $\mathtt{g}.\mathtt{p}$;
2. if $\mathtt{g}.\mathtt{p} = \mathtt{p}$, determine the index j of owner($\mathtt{c}$) in $\mathcal{O}_\mathtt{p}$;
3. if $\mathtt{g}.\mathtt{p} = \mathtt{p}$, determine the set $\mathtt{g}.\mathcal{S}_{\text{share}}$ of processes that share $\mathtt{g}$;
4. complete the entries in $\mathbf{E}_\mathtt{p}$ that refer to $\mathtt{g}$.

We will not give pseudocode for `Lnodes_callback` here; we only hope to convince the reader that the information that `Iterate` supplies to the `Lnodes_callback`—i.e., the local leaf support set $\text{leaf supp}_\mathtt{p}(\mathtt{c})$ for each point $\mathtt{c}$ in the closed locally relevant partition $\overline{\mathcal{P}_\mathtt{p}}$—is sufficient to accomplish the above listed tasks.

1. Determine $\mathtt{g}.\mathtt{p}$. The policy that defines owner($\mathtt{c}$) (6.2) guarantees that $\mathtt{c}$ and its nodes will be owned by a leaf in the partition of the first process $\mathtt{q}$ such that $\overline{\Omega_\mathtt{q}}$ intersects Dom($\mathtt{c}$). This means that each process $\mathtt{p}$ that references $\mathtt{c}$ can determine the processes that own all of the nodes it references, even if $\text{leaf supp}_\mathtt{p}(\mathtt{c})$ is incomplete

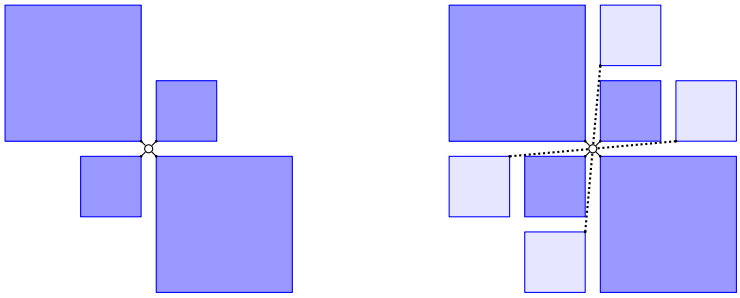

FIG. 6.2. *Because of the 2:1 condition,* `Reconstruct_remote` *(Algorithm 6.4) can use the octants in* leaf supp(c) *(left) to reconstruct remotely referencing leaves (right).*

(see Algorithm 6.3).

Algorithm 6.3: `Determine_owner_process` (point c)

Result : if $\mathtt{c} \in \mathcal{P}_\Omega$, the process that owns c and its global nodes.

1: **for** $\mathtt{e} \in \{\mathtt{c}\} \cup \text{part}(\mathtt{c})$ **such that** $\dim(\mathtt{e}) = 0$ **do** *[this set always contains one point]*
2: **return** $\min\{\text{locate}(\mathtt{a}) : \mathtt{a} \in \text{atom supp}(\mathtt{e})\}$

2. If $\mathtt{g}.\mathfrak{p} = \mathfrak{p}$*, determine* owner(c). Suppose $\text{owner}(\mathtt{c}) = \mathtt{o} \in \mathcal{O}_\mathfrak{p}$: o and c intersect, $\overline{\text{Dom}(\mathtt{o})} \cap \text{Dom}(\mathtt{c}) \neq \emptyset$. By definition (5.4), c must be in $\mathcal{P}_\mathfrak{p}$, so by Proposition 5.2, $\text{leaf supp}_\mathfrak{p}(\mathtt{c}) = \text{leaf supp}(\mathtt{c})$. Therefore, owner(c) will be in $\text{leaf supp}_\mathfrak{p}(\mathtt{c})$, and its index in $\mathcal{O}_\mathfrak{p}$ was calculated by `Iterate`, so we can set $\mathtt{g}.i$ equal to that index for each global node g located at c.

3. If $\mathtt{g}.\mathfrak{p} = \mathfrak{p}$*, determine* $\mathtt{g}.\mathcal{S}_{\text{share}}$. We use both Proposition 5.2 and the 2:1 balance condition to design an algorithm called `Reconstruct_remote` to reconstruct the octant data for all leaves that remotely reference (6.1) the point c and its nodes (Algorithm 6.4, Figure 6.2). By locating the processes that overlap the octants in $\text{leaf supp}_\mathfrak{p}(\mathtt{c})$ and the octants returned by `Reconstruct_remote`(c, $\text{leaf supp}_\mathfrak{p}(\mathtt{c})$), process $\mathfrak{p}$ can determine all processes that reference c's nodes.

Algorithm 6.4: `Reconstruct_remote` (point c, octant set leaf supp(c))

Input : the leaf support set leaf supp(c) (5.4).
Result : the set $\mathcal{R}$ of all octants that are leaves that remotely reference c.

1: $\mathcal{R} \leftarrow \emptyset$
2: **for all** $\mathtt{e} \in \bigcup \text{bound}(\text{leaf supp}(\mathtt{c}))$ **do** *[for every leaf's boundary point . . .]*
3: **if** $\mathtt{c} \in \text{bound}(\mathtt{e})$ **then** *[. . . that is adjacent to* c *]*
4: **for all** $\mathtt{s} \in \bigcup \text{supp}(\text{child}(\mathtt{e}))$ **do** *[for every octant* s *adjacent to a child of* e *]*
5: **if not** $\mathtt{s} \in \bigcup \text{desc}(\text{leaf supp}(\mathtt{c}))$ **then** *[if* s *is not a descendant of a leaf]*
6: $\mathcal{R} \leftarrow \mathcal{R} \cup \{\mathtt{s}\}$ *[*s *remotely references* c *(6.1)]*
7: **return** $\mathcal{R}$

4. Complete the references to g *in* $\mathbf{E}_\mathfrak{p}$. For each leaf $\mathtt{o} \in \text{leaf supp}_\mathfrak{p}(\mathtt{c}) \cap \mathcal{O}_\mathfrak{p}$ `Iterate` provides the index j in $\mathcal{O}_\mathfrak{p}$ such that $\mathcal{O}_\mathfrak{p}[j] = \mathtt{o}$, so determining the values of k such that $\mathbf{E}_\mathfrak{p}[j][k]$ refers to the global nodes at point c is a matter of comparing the orientation of o and c relative to each other. For each leaf $\mathtt{r} \in \mathcal{O}_\mathfrak{p}$ that remotely references c and its nodes, by definition (6.1) there must be a point e such that

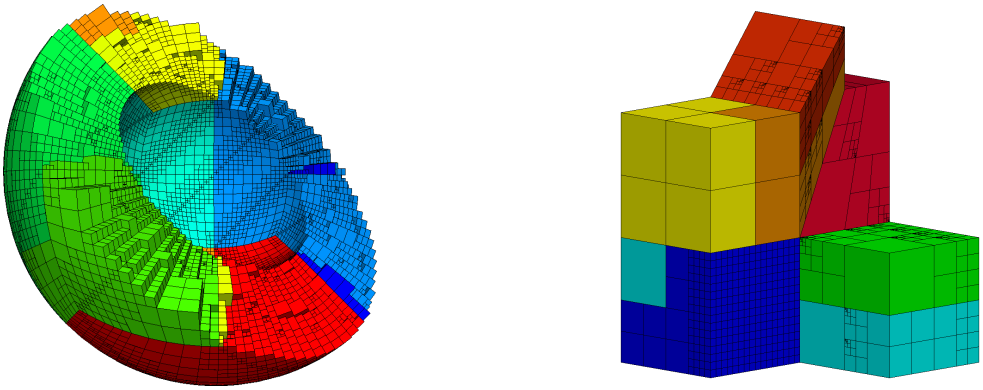

FIG. 7.1. *Example forests of octrees for nontrivial domain topologies. (left) A cutaway of a shell geometry, composed of 24 mapped octrees. (right) A collection of six rotated and mapped octrees connected in an irregular topology. Both show adhoc refinement patterns; a 2:1-balance condition has been enforced in the left hand plot, but not the right. Color indicates the partitions of different processes.*

$\mathtt{c} \in \text{bound}(\mathtt{e})$ and $\mathtt{r} \in \text{leaf supp}(\mathtt{e})$. The instance of `Lnodes_callback` called for the point `e` has the index j such that $\mathcal{O}_\mathtt{p}[j] = \mathtt{r}$ and can "link" it to `c`, so that the correct $\mathbf{E}_\mathtt{p}[j][\star]$ entries can be completed (see Remark 5.3).

The previously presented algorithm `Nodes` [6, Algorithm 21] produces data structures equivalent to those produced by `Lnodes` for $n = 1$. The ownership rule in `Nodes`—associating each node with a unique level-$(l_{\max}+1)$ octant (i.e., allowing the octant data structure to be more refined than an atom for storing nodes), and assigning ownership based on the process whose range contains that octant—is similar in principle to the ownership rule given in (6.2). `Nodes` does not have symmetric communication, however, because it does not construct the neighborhood $\text{leaf supp}_\mathtt{p}(\mathtt{c})$ when it creates a node at `c`, and so it cannot perform a calculation like `Reconstruct_remote`. Since it does not deduce the presence of remotely-sharing processes, `Nodes` requires a handshaking step, where the communication pattern is determined.

7. Performance evaluation. In this section we evaluate the efficiency and scalability of the algorithms presented in this work as they have been implemented in `p4est`. The parallel scalability is assessed on the Blue Gene/Q supercomputer JUQUEEN, which is configured with 28,672 compute nodes, each with 16 GB of memory and 16 cores, for a total of 458,752 cores. Additional concurrency is available through simultaneous multithreading: each core has two instruction/integer pipelines, and can issue one instruction to each of these pipelines per cycle, as long as they come from different threads. Where appropriate, we will compare results for 16, 32, and 64 MPI processes per node (`p4est` uses only MPI for parallelism). We have compiled the `p4est` library and executables with IBM's XL C compiler in version 12.1.

7.1. Search. To test the performance of `Search` (Algorithm 3.1), we consider the problem of identifying the leaves that contain a set of randomly generated points. We choose a spherical shell domain typical for simulations of earth's mantle convection, with inner radius $r = 0.55$ and outer radius $r = 1$, as illustrated in Figure 7.1 (left). For each test, we generate M points at random, independently and uniformly distributed in the cube containing the shell, and use `Search` as implemented by the `p4est` function `p8est_search` to identify the leaves that contain them.

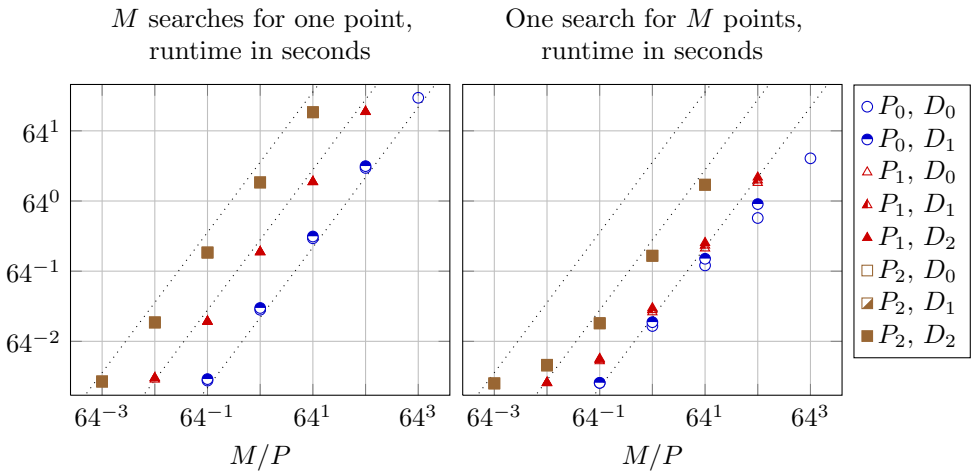

FIG. 7.2. *Scaling results for searching for M points in a shell domain using* `Search` *as implemented by* `p8est_search`. *We examine various values of M, P, and N. Three different values of P are used: $P_0 = 64$, $P_1 = 64^2$, and $P_2 = 64^3 = 262144$. Three different values of $N/P = D$ are used: $D_0 \approx 15$k, $D_1 \approx 122$k, and $D_2 \approx 979$k. (left) M separate calls of* `Search` *are used to find the M points. (right) One call of* `Search` *is used to find all M points. The dotted lines symbolize linear weak scaling; points on top of each other demonstrate the independence of the runtime from the local octant count D_i. The largest number of octants reached is 2.568×10^{11}.*

The mappings φ^t for the octrees (2.13) are given analytically for this domain. In the callback that we provide to `Search`, we have two tests to determine whether the mapped domain Dom(o) of an octant o contains a point x, one fast and inaccurate in the sense of allowing false positive matches, the other slower but accurate. In the accurate test, the mapping φ^t is inverted to get the preimage ξ of x, and a bounding box calculation determines whether $\xi \in \text{dom}(\mathtt{o})$. In the inaccurate test, the image $x_\mathtt{o}$ of the octant's center is computed, as well as an upper bound $r_\mathtt{o}$ on the radius of the bounding sphere of Dom(o), and we test whether $|x - x_o| \leq r_o$. In `Search` the accurate test is performed only when o is a leaf. We perform our tests on a series of forests with increasing numbers of leaves N, but with each forest refined so that the finest leaves are four levels more refined than the coarsest.

In Figure 7.2, we present the scaling results for our tests. Each of the P processes must determine which of the M points are in its partition. This means that each process must perform the inaccurate test at least M times. This is why, for fixed values of P, we see a scaling with $O(M)$. Indeed, the fraction of points that fall in a given processes partition is on average $1/P$, so for large values of P the majority of the runtime is spent on points that are not in the partition. This is why, in Figure 7.2, the number of leafs on a node N/P has so little effect on the runtime. When we take advantage of the algorithm's ability to search for multiple points simultaneously, however, the setup costs of the inaccurate test, such as computing the bounding radius r_o, can be amortized over multiple comparisons. Hence we see significant speedup when searching for multiple points simultaneously: in Figure 7.2, we see that for large values of P and for $M/P \geq 1$ the simultaneous search is roughly 64 times faster than searching for the same points individually.

7.2. Ghost. We test the performance of ghost layer construction as implemented by the `p4est` function `p8est_ghost`, on the irregular geometry shown in Figure 7.1

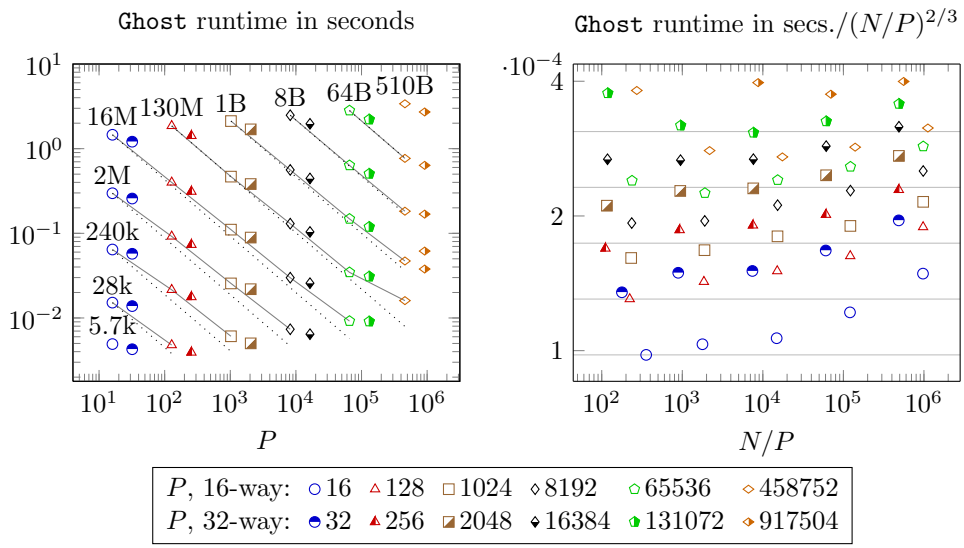

FIG. 7.3. *The scalability of ghost layer construction. The meshes used are described in the text: the largest number of leaf octants N is 5.1×10^{11}. (left) Runtime as a function of P: for 16-way process distribution, we compare strong scaling (solid lines) to ideal $O((N/P)^{2/3})$ scaling (dotted). The total number of leaves N in each mesh is indicated. (right) Runtime scaled by $(N/P)^{2/3}$ as a function of N/P. Weak-scaling is assessed by comparing the vertical distance between points: each grid line represents a 25% loss of weak-scaling efficiency relative to the ideal $O((N/P)^{2/3})$.*

(right). We again create a series of meshes with increasing N and four levels of difference between the coarsest and finest leaves. Our ghost layer construction uses `Find_range_boundaries` (Algorithm 4.2) to determine which processes' partitions border an octant `o`. When a partition $\Omega_\mathfrak{p}$ with $N_\mathfrak{p}$ leaves is well-shaped, we expect $O(N_\mathfrak{p}^{2/3})$ of those leaves to be on the boundary of $\Omega_\mathfrak{p}$, so we consider $O((N/P)^{2/3})$ to be ideal scaling. In the algorithm `Add_ghost` (Algorithm 4.1), which is called for each boundary leaf, $\log(P)$ work is performed to determine a set of potentially neighboring processes; the remaining leaves in the interior of the domain are skipped without calling `Add_ghost`, and so they should contribute very little to the runtime of `Ghost`. We therefore expect our performance to be $O((N/P)^{2/3} \log P)$.

In Figure 7.3, we give plots for assessing the strong- and weak-scalability of ghost layer construction, relative to the ideal $O((N/P)^{2/3})$ scaling. (For almost all problems, assigning 64 processes per node was slower than 32, so we omit this data from the figure.) We see good strong-scalability for $16 \le P \le 65\text{k}$ and $N/P \ge 1\text{k}$. For the full machine, when $P = 459\text{k}$ and $P = 918\text{k}$, the communication latency and the small amount of $O(P)$ workspace and work in the implementation (two scans of arrays of 32-bit integers) limits the efficiency for $N/P \le 10\text{k}$. In the weak-scaling plot, for the largest values of N/P, we see that the relative efficiency (the efficiency of $(8N, 8P)$ relative to (N, P)) improves slightly as N and P increase, which suggests that we are seeing $O((N/P)^{2/3} \log P)$ scaling asymptotically.

7.3. Serial comparison of `Lnodes` and `Nodes`. For polynomial degree $n = 1$, the data structures constructed by `Nodes` [6, Algorithm 21] and `Lnodes` (Algorithm 6.2) are essentially equivalent. For a general forest of octrees on a single process, both have $\mathcal{O}(N \log N)$ runtimes. While `Nodes` uses repeated binary searches and hash table

TABLE 7.1
Serial performance comparison of `Nodes` *(top) and* `Lnodes` *(bottom) for* $n = 1$*, as implemented by the* `p4est` *functions* `p8est_nodes` *and* `p8est_lnodes`*, on a series of single-octree forests.*

N	runtime (ms)	instructions	branch misses	cache misses
4.6×10^3	9.5×10^0	4.3×10^7	2.1×10^5	2.2×10^4
	1.0×10^1	3.7×10^7	5.3×10^4	1.1×10^4
3.9×10^4	8.6×10^1	4.2×10^8	1.7×10^6	2.2×10^5
	4.0×10^1	3.1×10^8	3.6×10^5	5.1×10^4
3.2×10^5	8.4×10^2	3.7×10^9	1.3×10^7	4.8×10^6
	3.5×10^2	2.5×10^9	2.7×10^6	4.5×10^5
2.6×10^6	8.0×10^3	3.3×10^{10}	1.0×10^8	6.1×10^7
	2.8×10^3	2.0×10^{10}	2.2×10^7	5.4×10^6

queries and insertions, `Lnodes` uses `Iterate` (Algorithm 5.3) to recursively split the forest and operates on subsets of leaves. This divide-and-conquer approach should make better use of a typical cache hierarchy. In this subsection, we present a small experiment that confirms this fact.

The experiment is conducted on a single octree using a single process. We again create a series of meshes with increasing N and four levels of difference between the coarsest and finest leaves. For each forest in the series, we have three programs: one that calls `Nodes`, one that calls `Lnodes`, and one that calls neither. We use the Linux utility `perf`[6] to estimate the number of instructions, cache misses, and branch prediction misses in each program, calling each program 30 times to compensate for the noise in `perf`'s sampling. The averages of the events from the program calling neither routine is subtracted from the other two averages, giving an estimate of the events that can be attributed to the two routines.

The experiment is performed on a laptop with two Intel Ivy Bridge Core i7-3517U dual core processors. Each core has a 64 kB on-chip L1 cache, a 256 kB L2 cache, and each processor has a 4 MB L3 cache: `perf` counts L3 cache misses. The `p4est` library and the executable are compiled by `gcc` 4.6.4 with `-O3` optimization.

The results of the experiment are given in Table 7.1. The table shows that the advantages of `Lnodes` over `Nodes` in terms of the number of instructions and the number of branch misses do not grow much with N, but the advantage in terms of cache misses grows from a factor of 2 on the smallest problem size to a factor of 11 on the largest.

7.4. Parallel scalability of `Lnodes`. In the previous subsection we compared the per-process efficiency of `Lnodes` and `Nodes`. Here we compare their parallel scalability on the same series of test forests used to test `Ghost` above.

In Figure 7.4 (top), we show the runtimes of `Lnodes` for $n = 1$. As discussed in Section 5.4, the implementation of `Iterate` has been optimized for large values of N/P: this optimization requires $O(l_{\max})$ workspace and setup time. The weak-scaling plot shows that the optimization is effective, in that for $N/P \geq 10$k and $P \leq 262$k the weak-scalability is nearly ideal, and that the absolute runtime is small (20 seconds for $1M$ leafs/process). The optimization requires redudant work, however, and this

[6] `https://perf.wiki.kernel.org`

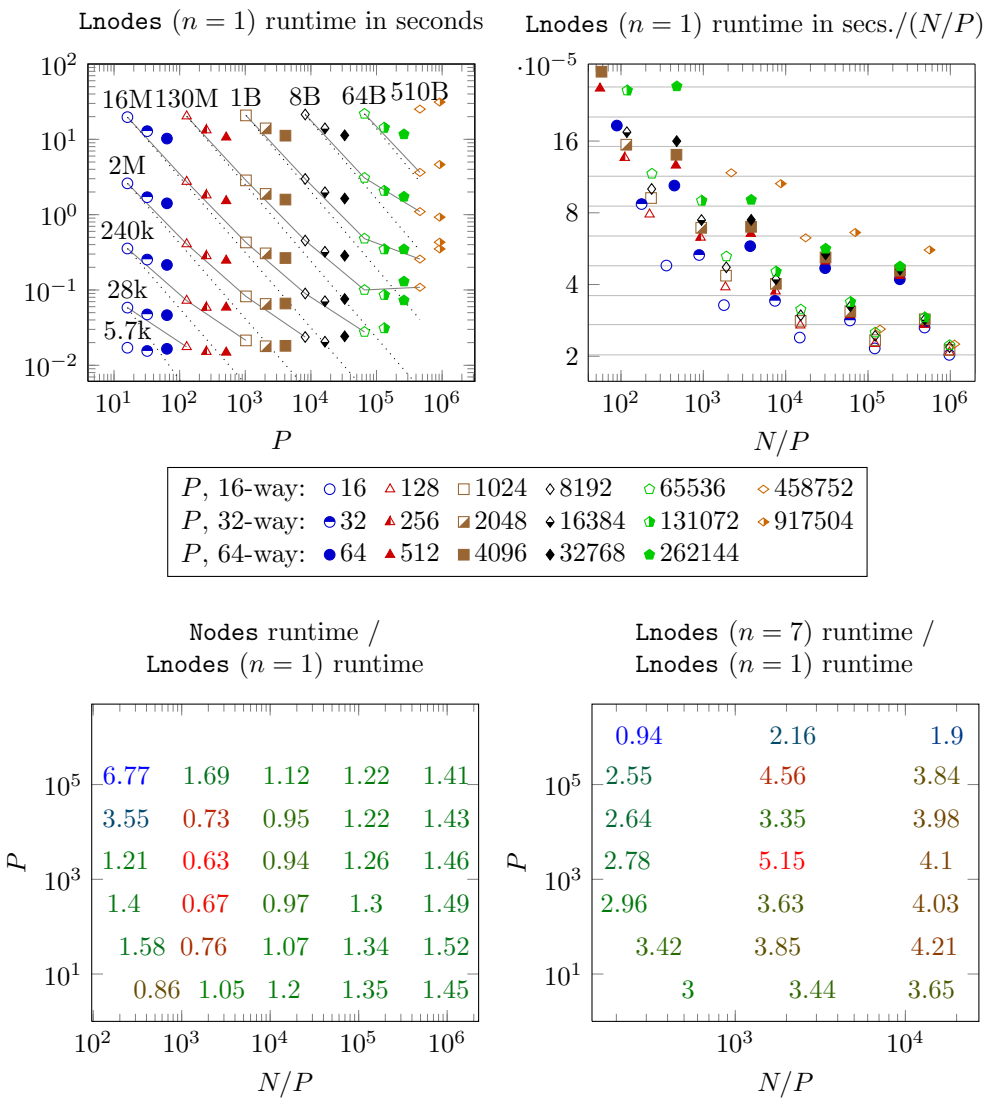

FIG. 7.4. *The parallel scalability of the* `Lnodes` *algorithm, as implemented by the* `p4est` *function* `p8est_lnodes`. *(top) Runtimes for* $n = 1$. *(top left) Runtime as a function of* P, *comparing strong scaling (solid lines) to ideal* $O(N/P)$ *scaling (dotted). The total number of leaves* N *in each mesh is indicated. (top right) Runtime scaled by* N/P *as a function of* N/P. *Weak-scaling is assessed by comparing the vertical distance between points: each grid line represents a* 25% *loss of weak-scaling efficiency. (bottom left) The speedup of* `Lnodes` *versus* `Nodes` *as implemented by* `p8est_nodes` *is shown for the same meshes as above. The color scale indicates whether* `Lnodes` *performs better (blue) or worse (red) than* `Nodes`. *(bottom right) The runtime for* $n = 7$, *scaled by the runtime for* $n = 1$, *with an analogue meaning of the colors.*

affects the efficiency for $N/P < 1$k. The strong-scaling plot shows good scalability for $P \leq 262$k and $(N/P) > 1$k, and in this range the algorithm benefits from 32 and 64 processes per node as well. As in the scaling for ghost layer construction, the communication latency and the small amount of $O(P)$ work in the implementation finally limit the scalability for the smallest meshes that were timed on the full machine.

In the same figure (bottom left) we compare the runtimes for `Lnodes` for $n = 1$ to the runtimes of `Nodes` [6, Algorithm 21]. For most tests, `Lnodes` is faster than `Nodes`: although the relative advantage is smaller on the Blue Gene/Q architecture of JUQUEEN than on the Ivy Bridge architecture used in the serial test, we still see the advantage increasing as N/P increases, which is suggestive of better cache performance. The communication pattern of `Lnodes`, consisting of one allgather and one round of point-to-point communication, is more scalable than the communication pattern of `Nodes`, which includes a handshake component, hence the better performance of `Lnodes` for small values of N/P and large values of P.

Finally, Figure 7.4 also compares the scalability of `Lnodes` for higher polynomial orders to the scalability for $n = 1$ (bottom left). We see that the runtime to construct 7th-order nodes is never more than six times the runtime to construct 1st-order nodes, even though there are 64 times as many element nodes and roughly 500 times as many global nodes.[7] For large values of P the communication costs, which do not increase significantly with n, dominate the runtime, so that the cost of constructing high-order nodes is essentially the same as 1st-order nodes.

8. Conclusion. In this work, we introduce new recursive algorithms that operate on the distributed forest-of-octrees data structures that the `p4est` software defines and uses to support scalable parallel AMR. The algorithms developed here exploit a recursive space partition from a topological point of view. They constitute `p4est`'s high-level reference interface, which is designed to be used directly from third-party numerical applications.

With the `Search` algorithm, we demonstrate how to efficiently traverse a linear octree downward from the root, even though the flat storage of leaves has no explicit tree structure. This search operation is in some sense purely hierarchical: a similar search could be performed even if the nodes and leaves of the tree were not interpreted as a space partition in $\mathbb{R}^d$.

As a component of the `Ghost` algorithm, we propose a recursive algorithm for determining the intersections between lower-dimensional boundary cubes and ranges of leaves that are specified only by the first and last leaves in the range. This algorithm is notable in that, while the procedure is recursive on the implicit octree structure, the result that it computes—a set of intersections—is purely topological in nature.

In the `Iterate` algorithm, we present a method of performing callback-based iteration over leaves and leaf boundaries that construct local topological information for the callback on the fly. This procedure combines aspects of the two previous algorithms: it involves recursion over the octree hierarchy and recursion over topological dimension. The divide-and-conquer nature of the algorithm makes better use of the cache hierarchy than approaches to iteration that rely on repeated searches through the array of leaves, as we demonstrate in practice.

We use `Iterate` in the construction of fully-distributed higher-order C^0 finite element nodes in the algorithm `Lnodes`. The topological information provided by `Iterate` simplifies the handling of non-conformal interfaces, and provides sufficient information to allow for node assignments to be made without communication, and for the communication pattern between referencing processes to be determined without handshaking. In practice, this gives us good scalability, which we have demonstrated to

[7] The number of global nodes depends on the forest topology and the refinement pattern. For a single octree with uniform refinement, the number of global nodes is asymptotically equivalent to n^3N, in which case the number of 7th-order nodes would be 343 times the number of 1st-order nodes. Because of non-conformal elements, however, we see a higher ratio.

nearly a half million processes on the JUQUEEN supercomputer. The implementation has been tuned for granularities of a thousand leaves per MPI process and above, and in this range we see good scalability, although room for improvement remains for smaller granularities.

The scalability of `Lnodes` that we have demonstrated is important for more applications than just higher-order finite element nodes, because the data structures returned by the `Lnodes` algorithm can also serve as the basis for converting a linear forest of octrees into an unstructured mesh adjacency graph. `Lnodes` includes all of the communication necessary for this conversion, so the same scalability should be achievable by third-party numerical codes that use `Lnodes` (or a similar approach based on `Iterate`) to interface `p4est` with their own mesh formats.

Reproducibility. The algorithms presented in this article are implemented in the `p4est` reference software [4]. `p4est`, including the programs used in the performance analysis presented above, is free and freely downloadable software published under the GNU General Public License version 2, or (at your option) any later version.

Acknowledgments. The first author thanks the U.S. Department of Energy for support by the Computational Science Graduate Fellowship (DOE CSGF) and by the Office of Science (DOE SC), Advanced Scientific Computing Research (ASCR), Scientific Discovery through Advanced Computing (SciDAC) program, under award number DE-FG02-09ER25914. The second author is supported by the Hausdorff Center for Mathematics (HCM) at Bonn University and the Transregio 32 research collaborative, both funded by the German Research Foundation (DFG).

The authors gratefully acknowledge the Gauß Centre for Supercomputing (GCS) for providing computing time through the John von Neumann Institute for Computing (NIC) on the GCS share of the supercomputer JUQUEEN at Jülich Supercomputing Centre (JSC). GCS is the alliance of the three national supercomputing centres HLRS (Universität Stuttgart), JSC (Forschungszentrum Jülich), and LRZ (Bayerische Akademie der Wissenschaften), funded by the German Federal Ministry of Education and Research (BMBF) and the German State Ministries for Research of Baden-Württemberg (MWK), Bayern (StMWFK) and Nordrhein-Westfalen (MIWF).

The authors are indebted to three anonymous reviewers, whose remarks led to significant improvements in the final form of this paper, and to Jose A. Fonseca and Johannes Holke for their editorial help.

REFERENCES

[1] V. Akçelik, J. Bielak, G. Biros, I. Epanomeritakis, A. Fernandez, O. Ghattas, E. J. Kim, J. Lopez, D. R. O'Hallaron, T. Tu, and J. Urbanic, *High resolution forward and inverse earthquake modeling on terascale computers*, in SC03: Proceedings of the International Conference for High Performance Computing, Networking, Storage, and Analysis, ACM/IEEE, 2003. Gordon Bell Prize for Special Achievement.

[2] W. Bangerth, C. Burstedde, T. Heister, and M. Kronbichler, *Algorithms and data structures for massively parallel generic adaptive finite element codes*, ACM Transactions on Mathematical Software, 38 (2011), pp. 14:1–14:28.

[3] W. Bangerth, R. Hartmann, and G. Kanschat, *deal.II – a general-purpose object-oriented finite element library*, ACM Transactions on Mathematical Software, 33 (2007), p. 24.

[4] C. Burstedde, *p4est: Parallel AMR on forests of octrees*, last accessed February 27, 2015. `http://www.p4est.org/`.

[5] C. Burstedde, G. Stadler, L. Alisic, L. C. Wilcox, E. Tan, M. Gurnis, and O. Ghattas, *Large-scale adaptive mantle convection simulation*, Geophysical Journal International, 192 (2013), pp. 889–906.

[6] C. Burstedde, L. C. Wilcox, and O. Ghattas, *p4est: Scalable algorithms for parallel adaptive mesh refinement on forests of octrees*, SIAM Journal on Scientific Computing, 33 (2011), pp. 1103–1133.

[7] P. Colella, J. Bell, N. Keen, T. J. Ligocki, M. Lijewski, and B. V. Straalen, *Performance and scaling of locally-structured grid methods for partial differential equations*, Journal of Physics: Conference Series, 78 (2007), pp. 1–13.

[8] P. Colella, D. T. Graves, N. Keen, T. J. Ligocki, D. F. Martin, P. W. McCorquodale, D. Modiano, P. O. Schwartz, T. D. Sternberg, and B. Van Straalen, *Chombo Software Package for AMR Applications. Design Document.*, Applied Numerical Algoirthms Group, NERSC Division, Lawrence Berkeley National Laboratory, Berkeley, CA, May 2007.

[9] K. Devine, E. Boman, R. Heaphy, B. Hendrickson, and C. Vaughan, *Zoltan data management services for parallel dynamic applications*, Computing in Science and Engineering, 4 (2002), pp. 90–97.

[10] J. Dreher and R. Grauer, *Racoon: A parallel mesh-adaptive framework for hyperbolic conservation laws*, Parallel Computing, 31 (2005), pp. 913–932.

[11] P. F. Fischer, G. W. Kruse, and F. Loth, *Spectral element methods for transitional flows in complex geometries*, Journal of Scientific Computing, 17 (2002), pp. 81–98.

[12] T. Goodale, G. Allen, G. Lanfermann, J. Masso, T. Radke, E. Seidel, and J. Shalf, *The Cactus framework and toolkit: Design and applications*, in Vector and Parallel Processing – VECPAR '2002, 5th International Conference, Springer, 2003.

[13] R. A. Haring, M. Ohmacht, T. W. Fox, M. K. Gschwind, D. L. Satterfield, K. Sugavanam, P. W. Coteus, P. Heidelberger, M. A. Blumrich, R. W. Wisniewski, et al., *The IBM Blue Gene/Q compute chip*, Micro, IEEE, 32 (2012), pp. 48–60.

[14] T. Isaac, C. Burstedde, and O. Ghattas, *Low-cost parallel algorithms for 2:1 octree balance*, in Proceedings of the 26th IEEE International Parallel & Distributed Processing Symposium, IEEE, 2012. `http://dx.doi.org/10.1109/IPDPS.2012.47`.

[15] *Forschungszentrum Jülich – JUQUEEN*. `http://www.fz-juelich.de/ias/jsc/EN/Expertise/Supercomputers/JUQUEEN/JUQUEEN_node.html`. Last accessed May 2, 2014.

[16] O. S. Lawlor, S. Chakravorty, T. L. Wilmarth, N. Choudhury, I. Dooley, G. Zheng, and L. V. Kalé, *ParFUM: a parallel framework for unstructured meshes for scalable dynamic physics applications*, Engineering with Computers, 22 (2006), pp. 215–235.

[17] J. Luitjens, M. Berzins, and T. C. Henderson, *Scalable parallel AMR for the Uintah multiphysics code*, in Petascale Computing Algorithms and Applications, D. A. Bader, ed., Chapman & Hall, 2008, pp. 67–81.

[18] P. MacNeice, K. M. Olson, C. Mobarry, R. de Fainchtein, and C. Packer, *Paramesh: A parallel adaptive mesh refinement community toolkit*, Computer physics communications, 126 (2000), pp. 330–354.

[19] J. P. May, *A concise course in algebraic topology*, University of Chicago Press, 1999.

[20] G. M. Morton, *A computer oriented geodetic data base; and a new technique in file sequencing*, tech. rep., IBM Ltd., 1966.

[21] C. D. Norton, J. Z. Lou, and T. A. Cwik, *Status and directions for the PYRAMID parallel unstructured AMR library*, in Proceedings of the 15th IEEE International Parallel and Distributed Processing Symposium (IPDPS), 2001, p. 120.

[22] S. Popinet, *Gerris: a tree-based adaptive solver for the incompressible Euler equations in complex geometries*, Journal of Computational Physics, 190 (2003), pp. 572–600.

[23] W. C. Rheinboldt and C. K. Mesztenyi, *On a data structure for adaptive finite element mesh refinements*, ACM Transactions on Mathematical Software, 6 (1980), pp. 166–187.

[24] R. S. Sampath, S. S. Adavani, H. Sundar, I. Lashuk, and G. Biros, *Dendro: Parallel algorithms for multigrid and AMR methods on 2:1 balanced octrees*, in SC'08: Proceedings of the International Conference for High Performance Computing, Networking, Storage, and Analysis, ACM/IEEE, 2008.

[25] C. Sert and A. Beskok, *Spectral element formulations on non-conforming grids: A comparative study of pointwise matching and integral projection methods*, Journal of Computational Physics, 211 (2006), pp. 300–325.

[26] J. R. Stewart and H. C. Edwards, *A framework approach for developing parallel adaptive multiphysics applications*, Finite Elements in Analysis and Design, 40 (2004), pp. 1599–1617.

[27] H. Sundar, R. Sampath, and G. Biros, *Bottom-up construction and 2:1 balance refinement of linear octrees in parallel*, SIAM Journal on Scientific Computing, 30 (2008), pp. 2675–2708.

[28] T. Tu, D. R. O'Hallaron, and O. Ghattas, *Scalable parallel octree meshing for terascale applications*, in SC '05: Proceedings of the International Conference for High Performance Computing, Networking, Storage, and Analysis, ACM/IEEE, 2005.

[29] L. C. Wilcox, G. Stadler, C. Burstedde, and O. Ghattas, *A high-order discontinuous*

Galerkin method for wave propagation through coupled elastic-acoustic media, Journal of Computational Physics, 229 (2010), pp. 9373–9396.

[30] M. Zhou, O. Sahni, K. D. Devine, M. S. Shephard, and K. E. Jansen, *Controlling unstructured mesh partitions for massively parallel simulations*, SIAM Journal on Scientific Computing, 32 (2010), pp. 3201–3227.

Appendix A. Proof of the correctness of `Find_range_boundaries` (Algorithm 4.2).

THEOREM A.1. *Given a range* $[\mathtt{f},\mathtt{l}]$*, where* $\mathtt{f}$ *and* $\mathtt{l}$ *are atoms with a common ancestor* $\mathtt{s}$*, and given a set of boundary indices* $\mathcal{B}_{\text{query}} \subseteq \mathcal{B}$*, Algorithm 4.2 returns the set* $\mathcal{B}_\cap(\mathtt{f},\mathtt{l},\mathtt{s}) \cap \mathcal{B}_{\text{query}}$ (4.4).

Proof. The proof is inductive on the refinement level, $\mathtt{s}.l$.

If $\mathtt{s}.l = l_{\max}$, then the only descendant of $\mathtt{s}$ is itself, so $\mathtt{s} = \mathtt{f} = \mathtt{l}$. Therefore $\bigcup \text{Dom}([\mathtt{f},\mathtt{l}]) = \text{Dom}(\mathtt{s})$ and $\mathcal{B}_\cap(\mathtt{f},\mathtt{l},\mathtt{s}) = \mathcal{B}$, so $\mathcal{B}_\cap(\mathtt{f},\mathtt{l},\mathtt{s}) \cap \mathcal{B}_{\text{query}} = B_{\text{query}}$. This is correctly returned on line 1.

Now suppose that `Find_range_boundaries` returns correctly if $l_{\max} \geq \mathtt{s}.l \geq m$, and suppose $\mathtt{s}.l = m-1$. Let $\mathtt{f} \in \text{desc}(\text{child}(\mathtt{s})[j])$ and $\mathtt{l} \in \text{desc}(\text{child}(\mathtt{s})[k])$: the set $\mathcal{I}$ defined in (4.7) is equal to $\{j,\dots,k\}$.

If $j = k$, then by Proposition 4.1, $\mathcal{B}_\cap(\mathtt{f},\mathtt{l},\mathtt{s}) = \mathcal{B}_\cap(\mathtt{f},\mathtt{l},\text{child}(\mathtt{s})[j]) \cap \mathcal{B}^j_\cap$. By the inductive assumption, line 4 returns

$$\mathcal{B}_\cap(\mathtt{f},\mathtt{l},\text{child}(\mathtt{s})[j]) \cap (\mathcal{B}^j_\cap \cap \mathcal{B}_{\text{query}}) = \mathcal{B}_\cap(\mathtt{f},\mathtt{l},\mathtt{s}) \cap \mathcal{B}_{\text{query}}. \tag{A.1}$$

Now suppose $j < k$. If the range $[\mathtt{f},\mathtt{l}]$ overlaps all of $\text{child}(\mathtt{s})[i]$, then the set $\mathcal{B}_\cap(\mathtt{f}_i,\mathtt{l}_i,\text{child}(\mathtt{s})[i])$ is equal to $\mathcal{B}$. This is the case if $j < i < k$, so the set $\mathcal{B}^1_{\text{match}}$ computed on line 5 is

$$\mathcal{B}_{\text{match}} = \bigcup_{j<i<k} \mathcal{B}_{\text{query}} \cap \mathcal{B}^i_\cap = \bigcup_{j<i<k} \mathcal{B}_{\text{query}} \cap (\mathcal{B}_\cap(\mathtt{f}_i,\mathtt{l}_i,\text{child}(\mathtt{s})[i]) \cap B^i_\cap). \tag{A.2}$$

This is also the case for $i = j$ if $\mathtt{f} = \mathtt{f}_j$, so on each branch of the condition on line 8 the set $\mathcal{B}^j_{\text{match}}$ is computed as

$$\begin{aligned} \mathcal{B}^j_{\text{match}} &= \mathcal{B}_\cap(\mathtt{f}_j,\mathtt{l}_j,\text{child}(\mathtt{s})[j]) \cap ((\mathcal{B}_{\text{query}} \cap \mathcal{B}^j_\cap) \backslash \mathcal{B}_{\text{match}}) \\ &= (\mathcal{B}_{\text{query}} \cap (\mathcal{B}_\cap(\mathtt{f}_j,\mathtt{l}_j,\text{child}(\mathtt{s})[j]) \cap \mathcal{B}^j_\cap)) \backslash \mathcal{B}_{\text{match}}. \end{aligned} \tag{A.3}$$

By the same reasoning, on each branch of the conditional on line 11, the set $\mathcal{B}^k_{\text{match}}$ is computed as

$$\mathcal{B}^k_{\text{match}} = (\mathcal{B}_{\text{query}} \cap (\mathcal{B}_\cap(\mathtt{f}_k,\mathtt{l}_k,\text{child}(\mathtt{s})[k]) \cap \mathcal{B}^k_\cap)) \backslash \mathcal{B}_{\text{match}} \backslash \mathcal{B}^j_{\text{match}}. \tag{A.4}$$

The union $\mathcal{B}_{\text{match}} \cup \mathcal{B}^j_{\text{match}} \cup \mathcal{B}^k_{\text{match}}$ is therefore equal to

$$\mathcal{B}_{\text{query}} \cap \bigcup_{j\leq i\leq k} \mathcal{B}_\cap(\mathtt{f}_i,\mathtt{l}_i,\text{child}(\mathtt{s})[i]) \cap \mathcal{B}^i_\cap = \mathcal{B}_{\text{query}} \cap \mathcal{B}_\cap(\mathtt{f},\mathtt{l},\mathtt{s}). \tag{A.5}$$

By induction, the proof is complete. ∎

Appendix B. Proof of the correctness of `Iterate_interior` (Algorithm 5.2).

Let the definitions in Section 5 be given. We prove the correctness of `Iterate_interior` (Algorithm 5.2) when the relevant set is $\overline{\mathcal{P}_\mathtt{p}}$. The proof for the case when $\mathcal{P}_\mathtt{p}$ is the relevant set is very similar.

THEOREM B.1. *Assume that the requirements for the arguments of Algorithm 5.2 are met. If* $\mathtt{c} \in \overline{\mathcal{P}_\mathtt{p}}$*, then* $\text{leaf supp}_\mathtt{p}(\mathtt{c})$ *is correctly computed. If there is a subset of* $\overline{\mathcal{P}_\mathtt{p}}$

whose domain is contained in $\mathrm{Dom}(\mathtt{c})$*, then the callback function is executed for all points in that subset.*

Proof. We first assert that if $\mathtt{c} \in \overline{\mathcal{P}_\mathfrak{p}}$, then its local leaf support $\mathrm{leaf\,supp}_\mathfrak{p}(\mathtt{c})$ is a subset of $\bigcup_i \mathbf{S}[i]$. By the definition of $\mathrm{leaf\,supp}(\mathtt{c})$, $\overline{\mathrm{Dom}(\mathtt{o})} \cap \mathrm{Dom}(\mathtt{c}) \neq \emptyset$. By Proposition 2.5, there is a point $\mathtt{e}$ in the closure set of $\mathtt{o}$, $\mathtt{e} \in \mathrm{clos}(\mathtt{o})$, such that $\mathrm{Dom}(\mathtt{e}) \subseteq \mathrm{Dom}(\mathtt{c})$ or $\mathrm{Dom}(\mathtt{c}) \subseteq \mathrm{Dom}(\mathtt{e})$. By the definition of the global partition set $\mathcal{P}_\Omega$, the former must be true: otherwise, $\mathtt{c}$ could not be in $\overline{\mathcal{P}_\mathfrak{p}} \subseteq \mathcal{P}_\Omega$. Therefore $\mathtt{o}$ cannot be less refined than $\mathtt{c}$, $\mathrm{level}(\mathtt{o}) \geq \mathrm{level}(\mathtt{c})$. By Proposition 2.6, there must be some support octant $\mathtt{s} = \mathrm{supp}(\mathtt{c})[i]$ such that $\mathtt{o} \in \mathrm{desc}(\mathtt{s})$. By the definition of $\mathbf{S}[i]$, it must contain $\mathtt{o}$. This proves the first assertion.

From here, we split the proof into two cases, $\dim(\mathtt{c}) = 0$, and $\dim(\mathtt{c}) > 0$.

Suppose $\dim(\mathtt{c}) = 0$. If $\mathtt{o} \in \mathrm{leaf\,supp}_\mathfrak{p}(\mathtt{c})$, then there is i such that $\mathtt{o} \in \mathbf{S}[i]$. By Proposition 2.8, $\mathtt{o}$ must be an ancestor of the atom $\mathrm{atom\,supp}(\mathtt{c})[i]$. Therefore $\mathtt{o}$ is added to $\mathcal{L}$ on line 18. Conversely, if $\mathtt{o}$ is added to $\mathcal{L}$ on line 18, then $\mathrm{atom\,supp}(\mathtt{c})[i]$ is a descendant of $\mathtt{o}$, and by definition its domain is in $\mathtt{o}$'s domain, $\overline{\mathrm{Dom}(\mathrm{atom\,supp}(\mathtt{c})[i])} \subseteq \overline{\mathrm{Dom}(\mathtt{o})}$. Because $\overline{\mathrm{Dom}(\mathrm{atom\,supp}(\mathtt{c})[i])} \cap \mathrm{Dom}(\mathtt{c}) \neq \emptyset$, it must be that $\overline{\mathrm{Dom}(\mathtt{o})} \cap \mathrm{Dom}(\mathtt{c}) \neq \emptyset$. Therefore $\mathtt{o}$ is a leaf in $\mathbf{S}[i] \subset \mathcal{O}_\mathfrak{p} \cup \mathbf{G}^d_\mathfrak{p}$ whose closure intersects $\mathtt{c}$, which matches the definition of $\mathrm{leaf\,supp}_\mathfrak{p}(\mathtt{c})$. Thus, if $\mathtt{c} \in \mathcal{P}_\Omega$, the set $\mathcal{L}$ computed is equal to $\mathrm{leaf\,supp}_\mathfrak{p}(\mathtt{c})$, and the callback will be executed on line 20 if and only if $\mathtt{c} \in \overline{\mathcal{P}_\mathfrak{p}}$.

Now suppose $\dim(\mathtt{c}) > 0$. Let L be the minimum level of a leaf $\mathtt{o} \in \cup_i \mathbf{S}[i]$. The remainder of the proof is inductive on the difference $\delta = L - \mathrm{level}(\mathtt{c})$.

Suppose $\delta = 0$, and let $\mathtt{o} \in \mathbf{S}[i]$ be a leaf with level $L = \mathrm{level}(\mathtt{c})$. Because $\mathtt{o} \subseteq \mathrm{supp}(\mathtt{c})[i]$ and because $\mathrm{level}(\mathrm{supp}(\mathtt{c})[i]) = \mathrm{level}(\mathtt{c})$ by definition, $\mathtt{o} = \mathrm{supp}(\mathtt{c})[i]$. Therefore $\overline{\mathrm{Dom}(\mathtt{o})} \cap \mathrm{Dom}(\mathtt{c}) \neq \emptyset$ and $\mathtt{o} \in \mathrm{leaf\,supp}_\mathfrak{p}(\mathtt{c})$. Because leaves do not overlap, it must be that $\mathbf{S}[i] = \{\mathtt{o}\}$. Therefore $\mathtt{o}$ is added to $\mathcal{L}$ on line 9.

Because of the 2:1 condition, all remaining leaves in $\mathrm{leaf\,supp}_\mathfrak{p}(\mathtt{c})$ have level $L+1$. Let $\mathtt{o} \in \mathbf{S}[j]$ be a leaf with level $L+1$. This implies that $\mathbf{S}[j] \neq \{\mathrm{supp}(\mathtt{c})[i]\}$, so the children of $\mathrm{supp}(\mathtt{c})[i]$ are assigned to $\mathbf{h}_i$ on line 12: $\mathtt{o}$ must be one of these children. On line 14, $\mathtt{o}$ is added to $\mathcal{L}$ if and only if $\overline{\mathrm{Dom}(\mathtt{o})} \cap \mathrm{Dom}(\mathtt{c}) \neq \emptyset$, which matches the definition of $\mathrm{leaf\,supp}_\mathfrak{p}(\mathtt{c})$. Therefore, if $\mathtt{c} \in \mathcal{P}_\Omega$, the constructed set $\mathcal{L}$ matches $\mathrm{leaf\,supp}_\mathfrak{p}(\mathtt{c})$, and the callback executes on line 20 if and only if $\mathtt{b} \in \overline{\mathcal{P}_\mathfrak{p}}$.

Now suppose the algorithm is correct for $0 \leq \delta < k$, and suppose $\delta = k$. There can be no i such that $\mathbf{S}[i] = \{\mathrm{supp}(\mathtt{c})[i]\}$, so the arrays $\mathbf{H}_i$ and octants $\mathbf{h}_i$ are computed on lines 11 and 12 for every i. Let $\mathtt{e}$ be in the child partition set $\mathrm{part}(\mathtt{c})$: $\mathtt{e}$ has level $\mathrm{level}(\mathtt{c}) + 1$. By definition, each octant in the support set $\mathrm{supp}(\mathtt{e})$ also has level $\mathrm{level}(\mathtt{c}) + 1$ and $\overline{\mathrm{Dom}(\mathrm{supp}(\mathtt{e})[i])} \cap \mathrm{Dom}(\mathtt{e}) \neq \emptyset$, which implies $\overline{\mathrm{Dom}(\mathrm{supp}(\mathtt{e})[i])} \cap \mathrm{Dom}(\mathtt{c}) \neq \emptyset$. Proposition 2.6 implies that there must be j and k such that $\mathrm{supp}(\mathtt{e})[i] = \mathrm{child}(\mathrm{supp}(\mathtt{c})[j])[k]$. Therefore $\mathrm{supp}(\mathtt{e})[i] = \mathbf{h}_j[k]$ and the set $\mathbf{S}_\mathtt{e}[i] = \mathbf{H}_j[k]$ is equal to $(\mathcal{O}_\mathfrak{p} \cup \mathbf{G}^d_\mathfrak{p}) \cap \mathrm{desc}(\mathrm{supp}(\mathtt{e})[j])$. This means that the arguments of the recursive call on line 25 are correct for each $\mathtt{e} \in \mathrm{part}(\mathtt{c})$. By the inductive assumption, the callback function is executed for the subset of $\overline{\mathcal{P}_\mathfrak{p}}$ whose domains are in $\mathrm{Dom}(\mathtt{c}) = \bigsqcup \mathrm{Dom}(\mathrm{part}(\mathtt{c}))$. By the principle of induction, the proof is complete. ∎

Appendix C. Asymptotic analysis of `Iterate` (Algorithm 5.3).

We first present the asymptotic analysis of the complexity of the algorithm in a single-process, single-octree setting.

THEOREM C.1. *Ignoring the time taken by the callbacks,* `Iterate` *executes in the worst case in* $O(N \log N)$ *time.*

Proof. The only operations in each instance of `Iterate_interior` that are not $O(1)$ are the $O(\log |\mathbf{S}[i]|)$ terms for the input arrays $\mathbf{S}[i]$. Each of these arrays is

associated with an octant $\mathrm{supp}(\mathtt{c})[i]$ that is an ancestor of a leaf. An octant $\mathtt{o}$ can only be in $\mathrm{supp}(\mathtt{c})$ if $\mathtt{c} \in \mathrm{bound}(\mathtt{o})$ and $\mathtt{c} = (\mathtt{o}, b)$ for some $b \in \mathcal{B}$. Therefore each ancestor octant can be associated with at most $|\mathcal{B}|$ terms with $O(\log |\mathbf{S}[i]|)$ complexity. An octree has $O(N)$ ancestors that are not leaves, so $O(N)$ searches are conducted. Each array $\mathbf{S}[i]$ contains a subset of leaves, so each $O(\log |\mathbf{S}[i]|)$ is $\mathcal{O}(\log N)$. We conclude that an upper bound on the running time is $O(N \log N)$. ∎

THEOREM C.2. *Ignoring callbacks,* `Iterate` *executes in $O(N)$ time on a uniformly refined octree.*

Proof. The leaves are all at the same level L, so $N = 2^{dL}$, and there are 2^{dl} nodes in level l of the tree. Because leaves are evenly distributed, each node at level l has $2^{d(L-l)}$ leaf descendants. Each node is associated with a bounded number of binary searches and calls to `Split_array`, each with logarithmic complexity in the number of leaves beneath it. So, ignoring leading coefficients, the time complexity is

$$\begin{aligned} \sum_{l=0}^{L-1} 2^{dl} \log 2^{d(L-l)} &= d \sum_{l=0}^{L-1} 2^{dl}(L-l) \\ &= d \sum_{l=0}^{L-1} \frac{2^{dL}}{2^{d(L-l)}}(L-l) \qquad \text{(C.1)} \\ [\hat{l} = L - l] \quad &= d 2^{dL} \sum_{\hat{l}=1}^{L} \frac{\hat{l}}{2^{d\hat{l}}} = d 2^{dL} O(1) = dO(N). \end{aligned}$$

Because the dimension d is fixed, `Iterate` runs in $O(N)$ time. ∎

A uniformly refined octree is just a regular grid, so the indices of neighbors follow a predictable rule: a linear-time algorithm can be achieved without a recursive algorithm and without searching through the leaf arrays. We outline a class of octrees which has no rule for neighboring indices, but for which `Iterate` still runs in linear time.

DEFINITION C.3 (Δ-uniform octrees). *A class of octrees is* Δ-uniform *if the difference* $(\max_{\mathtt{o} \in \mathcal{O}} \mathtt{o}.l - \min_{\mathtt{o} \in \mathcal{O}} \mathtt{o}.l)$ *is uniformly bounded by* Δ *for all octrees in the class.*

THEOREM C.4. `Iterate` *executes in $O(N)$ time on a class of Δ-uniform octree.*

Proof. Let $L = \max_{\mathtt{o} \in \mathcal{O}} \mathtt{o}.l$ and $l_{\min} = \min_{\mathtt{o} \in \mathcal{O}} \mathtt{o}.l$. For $l \min_{\mathtt{o} \in \mathcal{O}} \mathtt{o}.l$, $2^{d\ell}$ is now an upper bound on the number of nodes at level l, and for every l, $2^{d(L-l)}$ is an upper bound on the number of descendant leaves of a level l node. Therefore the $O(2^{dL})$ runtime for a uniform octree is an upper bound on the runtime of `Iterate`, while a lower bound on N is $2^{dl_{\min}} = 2^{d(L-\Delta)}$. Therefore $2^{dL} \leq 2^{d\Delta} N$, so the runtime of `Iterate` is $O(2^{d\Delta} N) = O(N)$. ∎

We now consider the `Iterate` algorithm in the multiple process, single octree setting, and derive bounds in terms of the local number of leaves $N_\mathtt{p}$ and the number of processes P. A key component of the above analysis for the serial runtime, that the number of ancestor nodes is $O(N)$, is no longer true in a parallel setting: the number of ancestors of the leaves in $\mathcal{O}_\mathtt{p} \cup \mathbf{G}^d_\mathtt{p}$ is not necessarily $O(N_\mathtt{p})$. Suppose $\mathtt{a}$ is the smallest common ancestor of every leaf in $\mathcal{O}_\mathtt{p} \cup \mathbf{G}^d_\mathtt{p}$ and $\mathtt{a}.l = \hat{l}$. The number of branches below $\mathtt{a}$ must be $O(N_\mathtt{p})$, so the analysis for the runtime after level $\hat{l}$ is the same as for a single process, substituting $\mathtt{a}$ for the root, so the time spent below $\mathtt{a}$ is $O(N_\mathtt{p} \log N_\mathtt{p})$ in general or $O(N_\mathtt{p})$ for a Δ-uniform tree. Thus an upper bound for the runtime is to add $O(\hat{l} \log N_\mathtt{p})$ to that time. We can bound $\hat{l}$ by $L = \max_{\mathtt{o} \in \mathcal{O}} \mathtt{o}.l$, and in the Δ-uniform case $L \in O(\log N)$. If we assume an even partitioning of the leaves, $N = PN_\mathtt{p}$, then

$L \in O(\log P + \log N_\mathfrak{p})$. The runtime for `Iterate` on an evenly distributed octree is thus $O((L + N_\mathfrak{p}) \log N_\mathfrak{p})$ in general and $O(\log P + N_\mathfrak{p})$ for Δ-uniform octrees.

Introducing multiple trees does not affect the analysis significantly: maintaining separate arrays for each tree can only reduce the sizes of the subarrays that are split by `Split_array`. Some time is taken to set up the calls to `Iterate_interior` for the interfaces between octrees, but this time is negligble, especially if the forest realizes the common use case $K \ll N$.